

PEOPLE'S DEMOCRATIC REPUBLIC OF ALGERIA
MINISTRY OF HIGHER EDUCATION AND SCIENTIFIC RESEARCH

University of Mohamed El-Bachir El-Ibrahimi - BordjBouArreridj

Faculty of Science and Technology

Department of Electromechanics

Discuss the graduation thesis in order to obtain the degree of MASTER

Fields: Automatic & Electrotechnics

Option 1: Automatic control and Industrial computer science

Option 2: Electrical control

Subject:

Design and Implementation of a Supervision Drone

Presented by : Saoud Selmane & Soukhal Hanane

Jury members:

<i>First name & Last name</i>	<i>Grade</i>	<i>Quality</i>	<i>Establishment</i>
<i>Mr. Abdelhamid Iratni</i>	<i>MCA</i>	<i>President</i>	<i>BBA University</i>
<i>Mr. Toufik Madani Layadi</i>	<i>MCA</i>	<i>Advisor</i>	<i>BBA University</i>
<i>Ms. Dounia Meradi</i>	<i>Phd</i>	<i>Co-Advisor</i>	<i>BBA University</i>
<i>Mr. Messaoud Mostefai</i>	<i>Pr</i>	<i>Examiner</i>	<i>BBA University</i>
<i>Mr. Abdelhak Benhaniche</i>	<i>MCA</i>	<i>Examiner</i>	<i>BBA University</i>
<i>Mr. Issam Meghlaoui</i>	<i>MCB</i>	<i>Guest</i>	<i>BBA University</i>

College year 2021/2022



Thanks

الحمد لله

الذي أعاننا وأنار لنا طريق العلم ووفقنا لإتمام عملنا المتواضع
والصلاة والسلام على
محمد سيد المرسلين وعلى آله وصحبه أجمعين إلى يوم الدين

*We thank God "ALLAH" all the strength that gave us the courage to
face this new field, and the strength to do this work,*

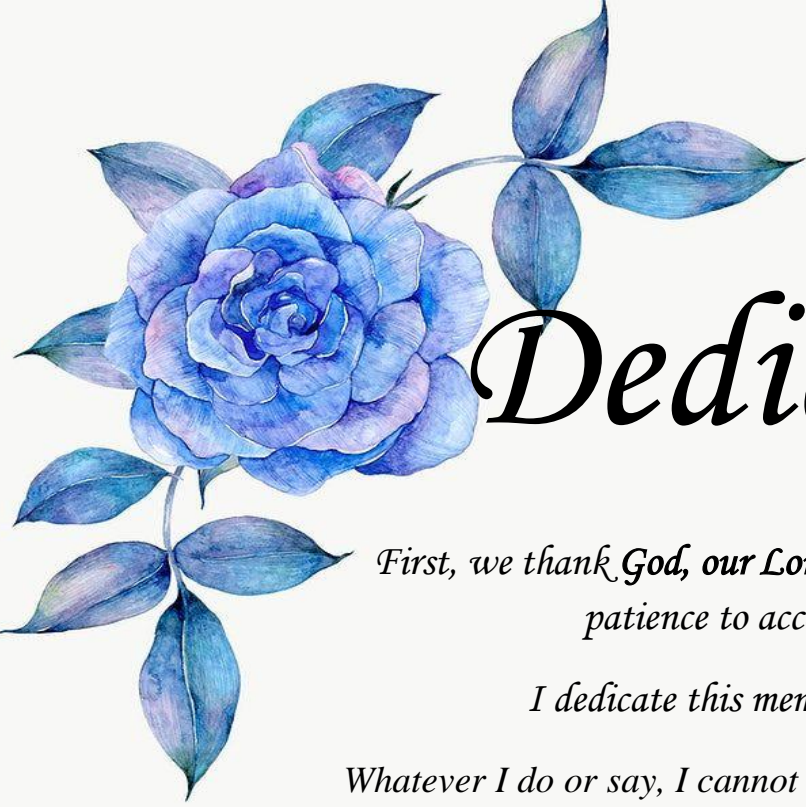
*We would like to thank the people who, thanks to them, we will never
be able to be there, our mothers and fathers. So is all of our family.*

*We would like to thank, in particular, to express our deepest gratitude
to our supervisors Mr. Layadi Toufik madani,
and Mrs. Meradi Dounia, who helped us a lot in the realization
of our drone and their precious advice.*

As we present our thanks to all the teachers of the electromechanical department.

Finally, we would like to thank all the people who helped us with our project.

Thank you to all our friends and colleagues.



Dedication

*First, we thank **God, our Lord**, who gave us the strength and patience to accomplish this work,*

*I dedicate this memoir to my **dear mother***

Whatever I do or say, I cannot thank you as I should. Your affection overwhelms me, your mercy guides me, and your presence by my side has always been the source of my strength in the face of various obstacles.

*To my **dear father***

You have always been by my side to support and encourage me. I hope this work reflects my gratitude and affection.

*To my dear brother **Adel** and to my dear sister **Asma***

May God reward you with health and happiness.

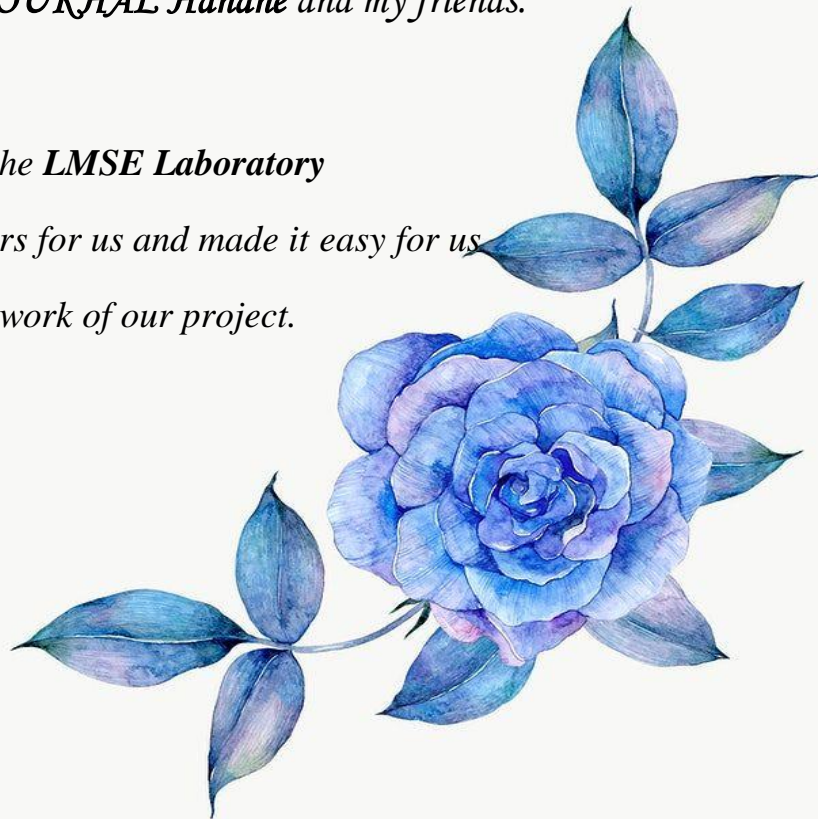
*To my binomial **SOUKHAL Hanane** and my friends.*

*TO the **LMSE Laboratory***

*Who always opened its doors for us and made it easy for us
to work of our project.*

SAOUD Selmane

« وقل ربي زدني علما »





Dedication

*First, we thank **God, our Lord**, who gave us the strength and patience to accomplish this work,*

*I dedicate this memoir to my **dear father** and **dear mother** who encouraged me to move forward and gave me all their great love, patience, and support so much during my course of study. And their sacrifices and prayers.*

I hope they will here accept my homage to my gratitude, which, however great, will never be equal to their tenderness and devotion.

*To my dear brother **Mohamed** and to my dear sister **Fairouz***

They always believed in me, and in their presence, I drew the will to continue. I wish them all success and happiness.

*To my binomial **SAOUD Selmane** and my friends.*

*TO the **LMSE Laboratory** Who always opened its doors for us and made it easy for us to work of our project.*

Without forgetting to thank all the teachers, whether they are primary, intermediate, secondary or university.

Thank you to everyone who helped me cross the horizon of my life.

SOUKHAL Hanane

« اللهم علمنا ما ينفعنا وانفعنا بما علمتنا وزدنا علما »

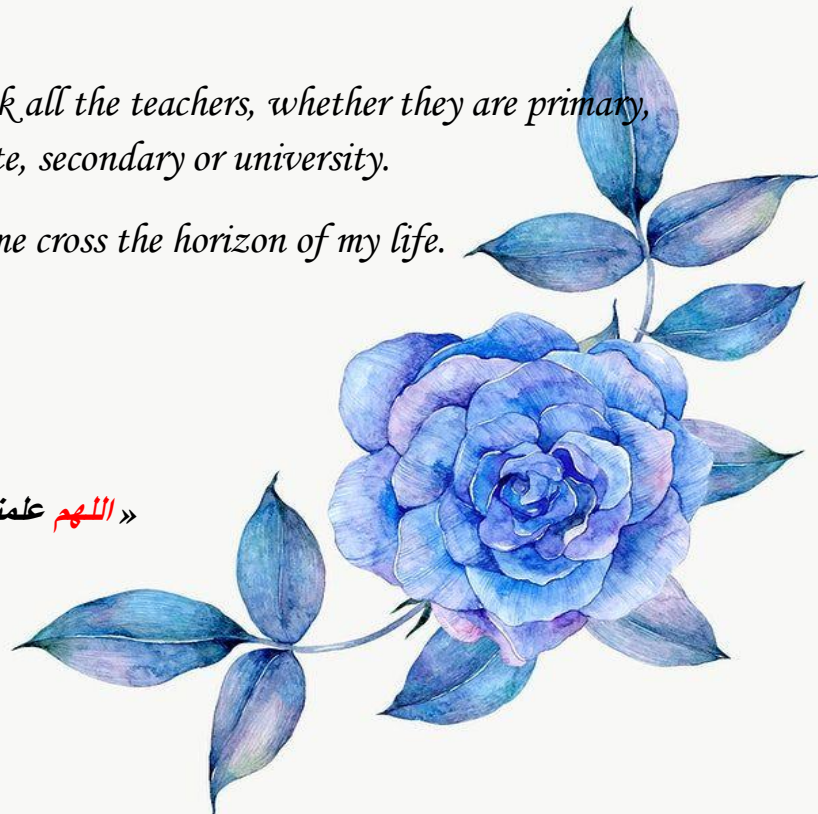


Table of content

Abstract	I
List of figure	II
List of tables	IV
Acronyms	V
List of symbols	VII
General introduction	1
Chapter 1: State of art of a drones	
1.1 Introduction	2
1.2 Definition of a drone	2
1.3 Classification of UAVs	2
1.3.1 Range classification	2
1.3.2 Aerodynamic configuration classification	3
1.3.3 Size and payload classification	6
1.3.4 Levels of Autonomy classification	8
1.4 Quad-copter concept	9
1.5 Quad-copter description	10
1.6 Research projects on quad-rotors	10
1.7 Quad-copter advantages	12
1.8 Application and usages of quad-copter	12
1.8.1 Photography	12
1.8.2 Military and law enforcement	13
1.8.3 Journalism	13
1.8.4 Delivery	13
1.8.5 Agriculture	14
1.8.6 Inspection of power lines	14
1.9 Challenges	15
1.10 Conclusion	16
Chapter 2: The modeling and control of the quad-copter	
2.1 Introduction	17
2.2 Quad-rotor modeling	17
2.2.1 The degrees of freedom of the quad-rotor	18
2.3 Quad-copter movements	18
2.3.1 Vertical movement	19
2.3.2 Rotation around the X-axis (Roll)	19
2.3.3 Rotation around the Y-axis (Pitch)	19
2.3.4 Rotation around the Z-axis (Yaw)	20
2.3.4 Rotation around the Z-axis (Yaw)	20
2.3.5 Translations on the X-axis	21
2.3.6 Translations on the Y-axis	21
2.4 Reference frames	21
2.4.1 The inertial frame	21
2.4.2 The body frame (mobile)	22

2.5	Rotation matrix	23
2.6	Dynamic model	24
	2.6.1 Relationship between Euler angles and angular velocities	25
	2.6.2 Rotor dynamics	26
2.7	State model	28
2.8	Discrete Time quad-rotor's model	30
2.9	Controller design	31
	2.9.1 Design of PD controller	31
	2.9.2 Design of DSMC with Gao's reaching law	33
	2.9.3 Design of DSMC with Power rate reaching law	33
2.10	Conclusion	34
Chapter 3: Simulation and conception of a drone		
3.1	Introduction	35
3.2	Part 1: Simulation results	35
	3.2.1 Nominal conditions	35
	3.2.2 The controllers' assessment in the presence of model mismatch and perturbations	38
3.3	Part 2: Design and conception	41
	3.3.1 Mechanical components	41
	3.3.3.1 Frame	41
	3.3.3.2 The propellers	42
	3.3.2 Electrical components	42
	3.3.2.1 Brushless motors	42
	3.3.2.2 Electronic Speed Controller	43
	3.3.2.3 Arduino card	43
	3.3.2.4 Module Nrf24L01	43
	3.3.2.5 Battery	43
	3.3.2.6 RC transmitter and receiver	44
	3.3.2.7 Ardupilot Mega (APM)	46
	3.3.3 Software used	47
	3.3.3.1 Mission planner	47
	3.3.3.2 MATLAB software	48
	3.3.3.3 Arduino IDE	49
	3.3.4 Quad-copter setup	49
	3.3.5 Mechanism of operation	52
	3.3.6 The general (complete) structure of our quad-rotor drone	55
	3.3.7 Components calibration	56
	3.3.7.1 ESC calibration	56
	3.3.7.2 IMU sensors calibration	57
	3.3.7.3 RC calibration	58
	3.3.8 Field tests	59
3.4	Conclusion	59
	General conclusion	60
	Bibliography	a
	Appendix	d

ملخص

في الآونة الأخيرة، أصبحت المركبات الجوية بدون طيار جزءًا مهمًا من الحياة اليومية للإنسان. تتراوح تطبيقات هذه الأنظمة من أبسطها إلى أكثرها حساسية. لتبسيط حياة الإنسان، يتم تغطية العديد من الخدمات بواسطة هذه الأنظمة. لذلك، يمكن استخدامها في الخدمات المدنية مثل الخدمات البريدية ولتوصيل الأطعمة. تسمح هذه الأنظمة في التطبيقات العسكرية بتنفيذ مهام معقدة. من خلال الاتصالات اللاسلكية، يمكن التحكم في هذه الطائرات بدون طيار عن بُعد على مسافات مختلفة (من بضعة أمتار إلى عشرات الآلاف من الكيلومترات). عادة ما تستخدم الطائرات الصغيرة بدون طيار محركات كهربائية بدون فرش. يتم تشغيلها بواسطة بطاريات الليثيوم بوليمر وأجهزة التحكم في السرعة الإلكترونية. يشكل استقلالية هذه الطائرات الصغيرة من دون طيار تحديًا يجب رفعه. يتعلق العمل الحالي بتصميم وتنفيذ طائرة بدون طيار رباعية المراوح مزودة بنظام قيادة. يتم التحكم فيه بواسطة جهاز تحكم لا سلكي. قبل تحقيق المركبة الجوية، تم إجراء العديد من اختبارات المحاكاة. فيما يتعلق بدمج تقنية التحكم في الطائرة بدون طيار المقترحة، تم اقتراح العديد من وجهات النظر للعمل المستقبلي.

Abstract

Recently, unmanned aerial vehicles have become an important part of everyday life for human being. The applications of these systems range from the most basic to the most sensitive. To simplify the human life, many services are covered by these systems. So, they can be used in civil services such as postal services and for delivering foods. In military applications these systems allow to realize sophisticated and complicated tasks. Through wireless communications, these unmanned planes can be controlled remotely at different ranges (from a few meters to tens of thousands of kilometers). Small drones usually use brushless electric motors. They are powered by lithium-polymer batteries and electronic speed controllers. The autonomy of these small drones is a challenge to lift. The present work concerns design and implementation of a quad-rotor drone equipped with an onboard command system. The main equipment used for the realization is an Ardupilot module (APM 2.8 version) controlled by radio controller. Before hardware realization many simulations tests have been performed. Concerning the integration of a control technique in the proposed drone several perspectives have been suggested to the future work.

Keywords: Quad-copter, brushless motors, ESC, Ardupilot, RC radio, PD, DSMC.

Résumé

Récemment, les véhicules aériens sans pilote sont devenus une partie importante de la vie quotidienne de l'être humain. Les applications de ces systèmes vont des plus basiques aux plus sensibles. Pour simplifier la vie humaine, de nombreux services sont couverts par ces systèmes. Ainsi, ils peuvent être utilisés dans les services publics tels que les services postaux et pour la livraison de nourriture. Dans les applications militaires, ces systèmes permettent de réaliser des tâches sophistiquées et compliquées. Grâce aux communications sans fil, ces avions sans pilote peuvent être contrôlés à distance à différentes distances (de quelques mètres à des dizaines de milliers de kilomètres). Les petits drones utilisent généralement des moteurs électriques sans balais. Ils sont alimentés par des batteries lithium-polymère et des contrôleurs de vitesse électroniques. L'autonomie de ces petits drones est un défi à relever. Le présent travail porte sur la conception et la réalisation d'un drone quadri-rotor équipé d'un système de commande embarqué. Le principal équipement utilisé pour la réalisation est un module Ardupilot (version APM 2.8) piloté par radio contrôleur. Avant la réalisation du matériel, de nombreux tests de simulations ont été effectués. Concernant l'intégration d'une technique de contrôle dans le drone proposé plusieurs perspectives ont été suggérées pour les travaux futurs.

Mots clés : Quad-copter, moteurs brushless, ESC, Ardupilot, radio RC, PD, DSMC.

List of figures

Chapter 01: State of art of drones

Figure 1. 1. Fixed-wing UAV	3
Figure 1. 2. Single-rotor of rotary-wing UAV	4
Figure 1. 3. Coaxial of rotary-wing UAV.....	4
Figure 1. 4. Tri-rotor of rotary-wing UAV	4
Figure 1. 5. Quad-rotor of rotary-wing UAV	5
Figure 1. 6. Multi-rotor of rotary-wing UAV	5
Figure 1. 7. Blimps UAV.....	5
Figure 1. 8. Flapping-wing UAV	6
Figure 1. 9. Full-Scale UAV	6
Figure 1. 10. Medium-scale UAV	7
Figure 1. 11. Small-scale UAV	7
Figure 1. 12. Mini UAV	7
Figure 1. 13. Micro UAV	8
Figure 1. 14. Kendoul's 11-level Framework	9
Figure 1. 15. Quad-copter description	10
Figure 1. 16. Quad-copter photography.....	13
Figure 1. 17. Quad-copter military and law enforcemen.....	13
Figure 1. 18. Quad-copter journalism.....	13
Figure 1. 19. Quad-copter delivery	14
Figure 1. 20. Quad-copter used for crop condition monitoring	14
Figure 1. 21. Quad-copter used for power line inspection monitoring	15

Chapter 02: The modeling and control of the quad-copter

Figure 2. 1. Six degrees of freedom of the quad-rotor	18
Figure 2. 2. Vertical translation movement	19
Figure 2. 3. Roll movement	19
Figure 2. 4. Pitch movement	20
Figure 2. 5. Yaw movement.....	20
Figure 2. 6. Translation on the X-axis.....	21
Figure 2. 7. Translation on the Y-axis.....	21

Figure 2. 8. The coordinate frames of the quad-rotor	23
Figure 2. 9. Passage of the marker R0 to the marker R1	24
Figure 2. 10. Equivalent electrical circuit.....	26
Figure 2. 11. Mechanical part of the motor	27
Figure 2. 12. Design controller scheme	31

Chapter 03: Simulation and conception of a drone

Figure 3. 1.(a)-(b)-(c) Evaluate the position according to the three axes X, Y, Z, (d) Evaluation of the yaw angle	36
Figure 3. 2 (a),(b) Evaluation the error of the roll and pitch angles.....	37
Figure 3. 3. Evaluate of the controls U_1 , U_2 , U_3 and U_4	37
Figure 3. 4. Disturbance d	38
Figure 3. 5. Disturbance dx	38
Figure 3. 6. (a)-(b)-(c) Evaluate the position according to the three axes X, Y, Z, (d) Evaluation of the yaw angle of the applied turbulence in interval $t \in 10; 15$ and $t \in 20; 25$	39
Figure 3. 7. (a), (b) Evaluation the error of the roll and pitch angles of the applied turbulence in interval $t \in 10; 15$ and $t \in 20; 25$	40
Figure 3. 8. Evaluate of the controls U_1 , U_2 , U_3 and U_4 of the applied turbulence in interval $t \in 10; 15$ and $t \in 20; 25$	41
Figure 3. 9. The 3-D tracking trajectory.....	41
Figure 3. 10. Battery Li-Polymer (Li-Po) 3S.....	44
Figure 3. 11. Radio control FlySky FS-i6.....	45
Figure 3. 12. Radio controller based on arduino and nRF24101	46
Figure 3. 13. Ardupilot Mega 2.8.....	47
Figure 3.14. Mission planner interface.....	48
Figure 3. 15. APM insulation layer	49
Figure 3. 16. APM Input and Output Connections	50
Figure 3. 17. Battery placement	51
Figure 3. 18. Mounted ESC and brushless motor	51
Figure 3. 19. Cnfiguration 1 connection diagram	53
Figure 3. 20. Configuration 2 Transmitter Connection Diagram.....	54
Figure 3. 21. Configuration 2 Receiver Connection Diagram.....	55
Figure 3. 22. The complete quad-copter structure	56
Figure 3. 23. Accelerometer Calibration	57
Figure 3. 24. Internal Compass Calibration.....	58
Figure 3. 25. RC Calibration.....	58
Figure 3. 26. Field tests	59

List of tables

Chapter 01: State of art of a drones

Table 1. 1. summary the quad-rotor drones family..... 10

Appendix D

Table D. 1. Quad-copter Parameters k
Table D. 2. Position Parameters of the PD Controller k
Table D. 3. Angle Parameters of the PD Controller k
Table D. 4. Parameters of DSMC with Gao’s reaching law controller l
Table D. 5. Parameters of DSMC with power rate reaching law controller l

Appendix E

Table E. 1. Components specification m

Acronyms

AAV	Autonomous Aerial Vehicles
APM	ArduPilot Mega
BLDC	BrushLess Direct Current
CSMC	Continuous-time Sliding Mode Control
DC	Direct Current
DFSMC	Discrete-time First-order Sliding Mode Control
DOF	Degrees Of Freedom
DSMC	Discrete-time Sliding Mode Control
EC	Environment Complexity
ES	External System
ESC	Electronic Speed Controller
ESI	External System Independence
FAA	Federal Aviation Administration
GCS	Ground Control Station
GPS	Global Positioning System
HALE	High-Altitude Long-Endurance
HI	Human Independence
IDE	Integrated Development Environment
IMU	Inertial Measurement Unit
Li-Po	Lithium-Polymer
LTE	Long-Term Evolution
LTI	Linear Time Invariant
MALE	Medium-Altitude Long-Endurance

MATLAB	MATh LABoratory
MAV	Micro Unmanned Aerial Vehicle
MC	MissionComplexity
MEMS	Micro Electronic Mechanical Systems
MUAV	Mini Unmanned Aerial Vehicle
NAV	Nano Air Vehicles
PD	Proportional-Derivative
PWM	Pulse Width Modulation
RC	Radio Control
RCS	Radio Control System
RT	Real Time
SA	Situational Awareness
SMC	Sliding Mode Control
SPI	Serial Peripheral Interface
SQL	Structured Query Language
TUAV	Tactical Unmanned Aerial Vehicle
UAV	Unmanned Aerial Vehicle
US	United States
USB	Universal Serial Bus
VSC	Variable Structure Control
VSS	Variable Structure System
VTOL	Vertical Take-Off and Landing

List of symbols

$R0$	The inertial frame
$O0$	Origin of the inertial frame
$X0, Y0, Z0$	Axes linked to the earth
$R1$	The body frame
$O1$	Origin linked to the body frame
$X1, Y1, Z1$	Axes linked to the body frame
x, y, z	Position vector of the quadrotor in the inertial frame
φ, θ, ψ	Roll angle, Pitch angle, Yaw angle
$\varphi_d, \theta_d, \psi_d$	Desired roll φ , Desired pitch θ , Desired yaw ψ
v_x, v_y, v_z	Speed of point $O1$ along the $X0, Y0, Z0$ axis
p, q, r	Instantaneous speed of rotation around the $X1, Y1, Z1$ axis
$R\varphi, R\theta, R\psi, Rot$	Roll rotation, Pitch rotation, Yaw rotation, Rotation Matrix
I	Inertia matrix
I_x, I_y, I_z	The area moments of inertia about the principle axes in the body frame
m	Mass of quadcopter
F_{ext}	External forces
P	Gravitational force of the earth
g	Acceleration of gravity on earth
F_p	Force generated by the rotation of the propellers
T	The total thrust force of the four propellers
f_i	The thrust force produced by the rotation of the propeller
b	Thrust coefficient
Γ_{ext}	The vector of external moments
Ω	The vector angular rates in the body-fixed frame
l	The distance between the center of gravity of the quadrotor

k	Drag coefficient
V_{EQ}	The effective voltage applied by the ESC
V_{EMF}	The back electromotive force
ω	The angular speed of the rotor
K_e	The electrical constant of the motor
L_{mot}, R_{mot}	The equivalent inductance and resistance of the motor
Γ_e, Γ_r	Electric torque provided by the motor, Torque due to air friction
V_B	The voltage available at the input
p	The pulse width at time t.
P_{max}, P_{min}	Maximum width of the pulse, Minimum pulse width
$s_i[k]$	Slotine surface in discrete time
$v_i[k]$	Virtual command in discrete time
$s_i[k + 1]$	Dynamic of the surface
$psign$	Pseudo-sign function
$u[k]$	Real commands
k_d	Derivative Gain
k_p	Proportional Gain

General introduction

Over the past decade, the robotics community has shown more interest in drones due to their significant advantages. Nowadays, in both military and civilian applications robotics becomes necessary to realize complicated tasks.

Quad-copter is an unmanned aerial vehicle for vertical take-off and landing, which has attracted a lot of attention in recent years and has become a research topic for many teams and laboratories. In this kind of vehicles, four propellers are used for lifting and propulsion. He made a significant contribution to simplify the setup by developing new components for the quad-copter design, in particular the development of the flight controller that served as the brain of the quad-copter. The aim of this work is to design a drone by integrating different methods of control.

This work is organized in three chapters:

In the first chapter, the technologies of drones are presented. Also many theoretical concepts, definitions, and concepts related to the field are given. Next various domains of research and ideas for the work being done in the field are explained.

The second chapter introduces the modeling and control of the quad-copter. We developed a case model that allows studying the dynamic evolution of angle, position, rotational speed, and four-wheel drive translation. Next, we apply PD control and discrete time sliding mode control to double the position and steering of the quad-copter. Finally, we show different results of simulations performed using Matlab/Simulink software.

The third chapter describes how we built the mechanical structure of a quad-copter, the stages of its realization, how radio control was achieved, and how we set up and calibrate the autopilot board. Simulation results, practical realization of the drone and perspectives are given.



Chapter 01

State of art of drones



1.1 Introduction

Recently, Autonomous Aerial Vehicles (AAV) has known a very active research and investment field due to recent technological developments. Thus, AAVs will be new tools for both civilian and military applications in the future. The main task of AAVs is to replace the human being in difficult tasks [1]. The private sector and universities incentivizing the creation of innovative vehicles (AAVs) will have to meet new technical requirements, That is, a combination of semi-flying in order to investigate specific objects in crowded environments, and aggressive flight at high speeds and accelerations, to reach remote areas in the shortest possible time. In particular, some universities have drawn their attention to the potential of verticals take-off and landing (VTOL) vehicles, where quad-copters are used in situations where conventional fixed-wing aircraft cannot operate properly [2].

1.2 Definition of a drone

A drone is an autonomous aircraft or an aircraft without a human pilot that uses aerodynamic forces to achieve vertical flight. It can be controlled remotely, autonomously, or semi-autonomously [3]. It may carry different payloads, enabling it to perform specific missions during flight times that may vary by capability. The use of UAVs has been developed for the first time in military applications such as surveillance and reconnaissance, as well as targeting platforms or as weapons. Then several civilian applications compete, especially in observing natural phenomena (avalanches, volcanoes, etc.), spraying pesticides on farmland, monitoring the environment (eg: pollution measurement) and road networks, maintaining infrastructure, etc. [4].

Today, several models of drones are available according to their fields of application and the mission granted. Among these models, there are fixed-wing drones, flapping-wing drones and vertical take-off and landing (rotary wing) aircraft ‘VTOL’: Vertical Take-off and Landing (VTOL) [5].

1.3 Classification of UAVs

UAVs can be classified in many ways, including according to their range of action, configuration, size, payload as well as autonomy.

1.3.1 Range classification

Drones can be divided into 7 different categories based on their maximum altitude and endurance, as can be shown below [6]:

- **High-Altitude Long-Endurance (HALE):** It can fly more than 15,000 meters and has an endurance of more than 24 hours. It mainly used for remote monitoring tasks.
- **Medium-Altitude Long-Endurance (MALE):** A maximum of 24 hours can fly between 5000-15000 m of altitude. These drones can also be used for surveillance.
- **Medium-Range or Tactical UAV (TUAV):** Flying at an altitude between 100 and 300 km, they can cover a large area. The systems that they use are simpler than those used by their HALE and MALE counterparts.
- **Close range UAV:** The range of their operation is 100 km. They are mainly used in civil applications such as power line inspection, crop spraying, traffic monitoring, and homeland security.
- **Mini UAV (MUAV):** They have a weight of about 20 kg and a range of about 30 km.
- **Micro UAV (MAV):** They have a maximum wingspan of 150 mm. In general, they are used indoors, where they are required to fly slowly and hover.
- **Nano Air Vehicles (NAV):** Their size is approximately 10 mm. They are usually used in swarms for purposes such as radar confusion. They can also serve as short range surveillance devices if they are equipped with a similar small camera.

1.3.2 Aerodynamic configuration classification

UAVs can be divided into four main categories based on their aerodynamic configuration. [6]:

Fixed-wing UAVs: Need a runway for take-off and landing. Can cruise at high speeds for a long time. They are used mainly in scientific applications such as meteorological reconnaissance and environment monitoring, as shown in Figure 1.1.



Figure 1. 1. Fixed-wing UAV

- **Rotary-wing UAVs:** The aircraft can take off and land vertically. It also can hover and fly with high maneuverability. Rotary-wing UAVs can be further divided into four groups [7]:

- **Single-rotor:** It is similar to helicopters where its configuration consists of a rotor at the top and another at the tail for its stability as can be shown Figure 1.2.



Figure 1. 2. Single-rotor of rotary-wing UAV

- **Coaxial:** Two rotors are mounted on the same shaft, rotating in opposite directions. As shown in Figure 1.3.

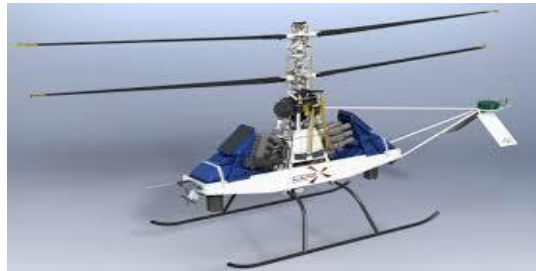


Figure 1. 3. Coaxial of rotary-wing UAV

- **Tri-rotors:** In the tri-rotor, two rotors spin oppositely at the front, and one rotates at the rear, whose orientation can be adjusted. The drone works much like a quadcopter, but the flight performance is not as good. Figure 1.4 shows this type of drones.



Figure 1. 4. Tri-rotor of rotary-wing UAV

- **Quad-rotor:** A cross-shaped configuration of four rotors is presented following Figure 1.5.



Figure 1. 5. Quad-rotor of rotary-wing UAV

- **Multi-rotor:** It is an unmanned aerial vehicle with six or eight rotors. Due to their large number of rotors, they are agile and can fly even when one of their motors malfunctions. Figure 1.6 demonstrates this type.



Figure 1. 6. Multi-rotor of rotary-wing UAV

By increasing the number of rotors on the UAV, the payload and height will be augmented, but it will also increase the size and power consumption.

- **Blimps UAVs:** They resemble balloons or airships, but they lift due to their helium-filled bodies. The blimps have large sizes and are very light. It is possible for them to fly at low speeds for a long time, as shown in Figure 1.7.



Figure 1. 7. Blimps UAV

- **Flapping-wing UAVs:** They are inspired by birds and flying insects. These drones have small wings and extremely low payload and endurance. On the other hand, they have low power consumption and can take off and land vertically. Such drones are still in development, as shown in Figure 1.8 [6].



Figure 1. 8. Flapping-wing UAV

1.3.3 Size and payload classification

UAVs can be divided into five main classes according to the size and payload of their payloads [8].

- **Full-Scale UAVs:** Figure 1.9 shows normal-sized vehicles. Even if a pilot is present, the vehicle is capable of autonomous flying. In flight tests and maneuvers that require complex skills, the pilot is there to assist. Such vehicles are also powerful, durable, and with the highest payload.



Figure 1. 9. Full-Scale UAV

- **Medium-scale UAVs:** For security missions, these are the vehicles of choice. Because they carry a relatively high payload of 10 kg, they are able to carry out heavy and high-quality navigation sensors, thus enabling independent flying. Figure 1.10 gives an example of a Medium Scale UAV used by the US Army.



Figure 1. 10. Medium-scale UAV

- **Small-scale UAVs:** These UAVs are primarily RC toys. Despite their lower payload of 2 to 10 kg, they are capable of carrying adequate quality navigation sensors. (Figure 1.11).displays an example of a small unmanned aerial vehicle.



Figure 1. 11. Small-scale UAV

- **Mini UAVs:** UAVs that can fly indoors and outdoors with a payload of less than 2 kilograms, which is enough to carry small and lightweight sensors. They are the most common test-bed UAVs in research due to their small size, low cost and ease of maintenance. Figure 1.12 illustrates a mini UAV.



Figure 1. 12. Mini UAV

- **Micro UAVs:** Because they are so small, they are mostly used indoors. Since they have a payload of less than 100 g, it is hard to add sensors for navigation and guidance. The research challenge regarding these micro UAVs is to design light-

weight navigation and guidance sensors. An example of a micro UAV is shown in Figure 1.13.



Figure 1. 13. Micro UAV

1.3.4 Levels of autonomy classification

Drones can also be classified according to their degree of autonomy National Institute of Standards and Technology published a framework used for the UAVs classification. This latter is defined by three indicators, according to their degree of autonomy, namely, Human independence (HI), Mission complexity (MC), and environment complexity (EC). This framework proposes five levels of autonomy [6]:

- **Level 1:** Operating these drones requires full human interaction because they are strictly remote-controlled. Tier 1 drones are primarily used for the least complex tasks.
- **Level 2:** Human interaction is still required, but can perform more complex tasks than tier 1 drones.
- **Level 3:** Level 3 features allow for autonomous navigation in certain identified environments where the pilot is prompted for engagement when needed.
- **Level 4:** Minimal human interaction is used in tasks where the environment is complex and dynamic, and the operator's reaction time may not be sufficient to properly navigate the UAV.
- **Level 5:** There is no human-drone interaction for performing tasks in the most complex environments. The literature claims that Class 5 UAVs do not currently exist and are the target of future research.

While the National Institute of Standards and Technology proposed a five-level classification framework valid for UAVs, Kendoul found it insufficient for classification of current UAVs and proposed an eleven-level framework, called Autonomy Levels for Unmanned Rotorcraft Systems [6], [8]. To classify UAVs, Kendoul used six metrics: External

System Independence (ESI), Environment Complexity (EC), Mission Complexity (MC), External System (ES), Situational Awareness (SA) and Real Time (RT) [6],[7]. The framework is shown in Figure 1.14.

LEVEL	LEVEL DESCRIPTOR	GUIDANCE	NAVIGATION	CONTROL	ESI	EC	MC
10	Fully Autonomous	Human-level decision-making, accomplishment of most missions without any intervention from ES (100% ESI), cognizant of all within the operation range.	Human-like navigation capabilities for most missions, fast SA that outperforms human SA in extremely complex environments and situations.	Same or better control performance as for a piloted aircraft in the same situation and conditions.	approaching 100% ESI	extreme environment	highest complexity all missions
9	Swarm Cognizance and Group Decision Making	Distributed strategic group planning, selection of strategic goals, mission execution with no supervisory assistance, negotiating with team members and ES.	Long track awareness of very complex environments and situations, inference and anticipation of other agents intents and strategies, high-level team SA.	Ability to choose the appropriate control architecture based on the understanding of the current situation/context and future consequences.	high level ESI	difficult environment	collaborative, high complexity missions
8	Situational Awareness and Cognizance	Reasoning and higher level strategic decision-making, strategic mission planning, most of supervision by RUAS, choose strategic goals, cognizance.	Conscious knowledge of complex environments and situations, inference of self/others intent, anticipation of near-future events and consequences (high fidelity SA).	Ability to change or switch between different control strategies based on the understanding of the current situation/context and future consequences.	mid level ESI	moderate environment	mid complexity, multi-functional missions
7	RT Collaborative Mission Planning	Collaborative mission planning and execution, evaluation and optimization of multi-vehicle mission performance, allocation of tactical tasks to each agent.	Combination of capabilities in levels 5 and 6 in highly complex, adversarial and uncertain environment, collaborative mid fidelity SA.	same as in previous levels (no-additional control capabilities are required)	low level ESI	simple environment	low level tasks
6	Dynamic Mission Planning	Reasoning, high-level decision making, mission driven decisions high adaptation to mission changes, tactical task allocation, execution monitoring.	Higher-level of perception to recognize and classify detected objects/events and to infer some of their attributes, mid fidelity SA.	same as in previous levels (no-additional control capabilities are required)	low level ESI	simple environment	low level tasks
5	RT Cooperative Navigation and Path Planning	Collision avoidance, cooperative path planning and execution to meet common goals, swarm or group optimization.	Relative navigation between RUAS, cooperative perception, data sharing, collision detection, shared low fidelity SA.	Distributed or centralised flight control architectures, coordinated maneuvers.	low level ESI	simple environment	low level tasks
4	RT Obstacle/Event Detection and Path Planning	Hazard avoidance, RT path planning and re-planning, event driven decisions, robust response to mission changes.	Perception capabilities for obstacle, risks, target and environment changes detection, RT mapping (optional), low fidelity SA.	Accurate and robust 3D trajectory tracking capability is desired.	low level ESI	simple environment	low level tasks
3	Fault/Event Adaptive RUAS	Health diagnosis, limited adaptation, onboard conservative and low-level decisions, execution of pre-programmed tasks.	Most health and status sensing by the RUAS, detection of hardware and software faults.	Robust flight controller, reconfigurable or adaptive control to compensate for most failures, mission and environment changes.	low level ESI	simple environment	low level tasks
2	ESI Navigation (e.g., Non-GPS)	Same as in Level 1	All sensing and state estimation by the RUAS (no ES such as GPS), all perception and situation awareness by the human operator.	Same as in Level 1	low level ESI	simple environment	low level tasks
1	Automatic Flight Control	Pre-programmed or uploaded flight plans (waypoints, reference trajectories, etc.), all analyzing, planning and decision-making by ES.	Most sensing and state estimation by the RUAS, all perception and situational awareness by the human operator.	Control commands are computed by the flight control system (automatic control of the RUAS 3D pose).	low level ESI	simple environment	low level tasks
0	Remote Control	All guidance functions are performed by external systems (mainly human pilot or operator)	Sensing may be performed by the RUAS, all data is processed and analyzed by an external system (mainly human).	Control commands are given by a remote ES (mainly human pilot).	0% ESI	lowest EC	lowest MC

Figure 1. 14. Kendoul's 11-level Framework

1.4 Quad-copter concept

The quad-copter is an aircraft that is a part of the helicopter family, or the multi-rotor family. It has many characteristics, including: mechanical simplicity of vertical take-off and landing, hovering, agility, which gives it many advantages compared to other aircraft [9].

1.5 Quad-copter description

A quad-copter is a rotating plane consisting of four motors located at the ends of four arms. Two rotors rotate clockwise and the other two counterclockwise. Each pair of propellers rotating in the same direction is placed on opposite ends of the arms branch. Thus, its movement is controlled by changing the angular velocity of each rotor to change the lift force and the torque generated by them. It is possible to make it move up and down, tilt it to the left, right, forward, or backward, and even rotate it on itself. It has six degrees of freedom, three rotational motions, and three transitional motions. These six degrees must be controlled using only four actuators, so it is an under-actuated system (the number of inputs is less than the number of outputs) [9],[11].

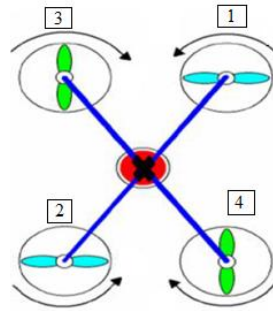

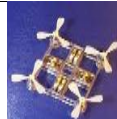










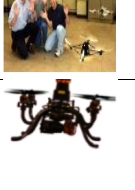






Figure 1. 15. Quad-copter description [5]

1.6 Research projects on quad-rotors

Table 1. 1. summary the quad-rotor drones family [12]

Project	University/ Organization	Year	Research studies	Design
V Ti	Dragan flyer	1998	- Commercial product.	
Mesicopter-I., Kroo	Stanford	2000- 2012	- Design and Manufacturing Techniques. - Control of Multiple UAVs for Persistent Surveillance.	
E. Altug	Uni. Pennsylvania	2002- 2012	- Yaw and height control using Visual feedback control techniques. -Obstacle avoidance using Catadioptric cameras.	
P. Pounds's thesis	ANU	2002-	- Dynamic modeling based on Newton-Euler Method. - Output tracking for quad-rotor-based	

X-4 Flyer, P., Pounds	FEIT, ANU	2014	aerial manipulators.	
P. Castillo's thesis, A. Dzul	Uni. Compiegne	2003-2015	- Dynamic modeling using Lagrange approach. - Precise measurement and prediction of position and orientation of the vehicle in the presence of external perturbation.	
Sarmac	Stanford	2004-2011	- Altitude and attitudes control in presence of wind. - Collision avoidance and control of the vehicle in aggressive maneuver utilizing combination of hybrid decomposition and reachable set theory.	
SarmacII				
Bouabdallah & Siegwart	EPFL	2004-2011	- Autonomous control of the vehicle in indoor environment. - Robust control of quad-rotor in presence of model uncertainties and external disturbances.	
F.B. Çamlica's thesis, C Özgen	Middle East Technical University, Turkey	2004-2014	- Hover control. - Trajectory tracking in presence of disturbance.	
Eryk Brian Nice's thesis and R. D'Andrea	Cornell University	2004-2015	- Nonlinear dynamic modeling and hover control. - Iterative learning controller for improving the performance of the vehicle in highly dynamic open-loop maneuver.	
M. Kemper's thesis	Uni. Oldenburg	2006-2009	- Robust control of quad-rotor respect to variable center of gravities. - Waypoint navigation and trajectory optimization.	
P.Tournier and J.P. How	MIT	2007-2015	- Autonomous control of quad-rotor by using visual serving method. -Control of variable-pitch quad-rotor.	
IARC Team Quadrotor	IARC Team - Virginia Tech. Uni.	2009	- Carrying payload.	
AVL's Micro Quad (J. Sean Humbert)	Univ. Maryland	2009-2015	- Robust visual navigation. - Robust stabilization and command tracking behavior in obstacle-laden environments	

Farshid Jafari Harandi	Azad University of Ghazvin	2010	- Outdoor navigation.	
CrazyFlie	CrazyFlie	2011	- Commercial product.	

1.7 Quad-copter advantages

The quad-copter offers real advantages over other configurations[5], [10]:

- A simpler control system.
- Less gyroscopic vibration.
- Increased stability.
- The reduced size and maneuverability of the drone allow it to maneuver in closed or open environments without hitting obstacles.
- Vertical take-off and landing are possible.
- The four motors are controlled solely by varying the rotational speed.
- Its dynamic is lower than that of a helicopter, so it requires less reaction time.
- A new design replaces the large helicopter rotor with four small ones, which reduces the store of kinetic energy and minimizes damage in case of an accident.

1.8 Applications and usages of quad-copter

Due to the quad-copters unique characteristics, such as their high maneuverability, small size, and relative ease of control, they have many uses and applications.

1.8.1 Photography

Images and videos are some of the most common outcomes of drone work. The services could include wedding and commercial photography, real estate marketing photography, or even filming for movies.



Figure 1. 16. Quad-copter photography

1.8.2 Military and law enforcement

Quad-copters are used in surveillance and reconnaissance missions by the armed forces and law enforcement agencies, as well as search and rescue missions in urban areas [5].



Figure 1. 17. Quad-copter military and law enforcement

1.8.3 Journalism

Drones and quad-copters are used by the media to report and verify information about flooding, protests, and wars[5].



Figure 1. 18. Quad-copter journalism

1.8.4 Delivery

An unmanned aerial vehicle (UAV) is used to transport packages, food, or medical supplies. Such drones are typically autonomous. The Federal Aviation Administration (FAA) proposed airworthiness criteria for type certification of delivery drones in November 2020,

with the objective of beginning commercial operations. Zepline, Wingcopter, and Amazon Prime Air were among the 10 companies selected for this type certification.



Figure 1. 19. Quad-copter delivery

1.8.5 Agriculture

The quad-copter is an interesting platform for agriculture and forestry since it can provide precise geographical information about the terrain to reduce human effort and perform accurate surveying, so the authors propose the quad-copter use [9].



Figure 1. 20. Quad-copter used for crop condition monitoring

1.8.6 Inspection of power lines

Powered aerial vehicles are mainly used to inspect high voltage power lines. In particular, drones have a lot of potential for automatic inspection, since they provide faster inspections and offer the same or better accuracy as helicopters. Therefore, the authors suggest inspecting power lines with quad-copters equipped with a color camera and thermal imaging (TIR) camera [9].



Figure 1. 21. Quad-copter used for power line inspection monitoring

1.9 Challenges

Quad-rotors are inherently unstable - stable hovering cannot be achieved by applying the same input to all four motors. Each quad-rotor's motor inputs have to be driven at a sufficiently high frequency which depending on its dynamic characteristics. The small size quad-rotor is more agile since its maximum angular acceleration is inversely proportional to its size, as shown in [13], [14].

As a consequence, high drive frequencies would be required to cope with the faster vehicle dynamics. In addition, smaller quad-rotors are less efficient because of their small rotor disc area, which decreases quadratically with their size. The following reasons explain why it can be difficult to identify the best quad-rotor configuration for a given task, since there are tradeoffs between flight time, agility, and sensors and software [13].

Four control inputs are needed to control quad-rotors six degrees of freedom, so they are under actuated. Free flight does not present a problem, since only four independent degrees of freedom need to be controlled. The problem is that quad-rotors cannot exert force, no matter what their orientation is, which means that they cannot interact with their surroundings. The problems risk can arise when taking off from a slope, for example, and ought to be taken into account during the take-off procedure [13], [15].

Hence, for interactions with the environment, the use of aerial vehicles with several axes of actuation is relatively common, such as helicopters [13], [16] and hexa-rotors equipped with inclined propellers [13], [17]. In addition, during agile flight close to the physical limits of a quad-rotor, the motors can become saturated, making it difficult to control all four degrees of freedom independently.

1.10 Conclusion

In this chapter, concept and classification of unmanned aerial vehicles and chose the type of quad-rotor have been presented. Then, the different applications of the quad-rotor drones are given. In addition their advantages have been explained. The modeling of this type of drones will be discussed in the next chapter.



Chapter 02

*The modeling
and control of
the quad-copter*



2.1 Introduction

A quad-copter experiment requires several control algorithms that can be used to create control laws; the disadvantage of these methods is that the aircraft performance will deteriorate if it moves away from its equilibrium point. Further, perturbations can destabilize these compounds. An adaptive system can be used to achieve stability in this situation.

In this chapter, the basic principles governing the operation of the four motors are presented, along with dynamic (or mathematical) modeling of the control of a four-engine system. In fact, in order to be able to control and drive the drone, which is an under-actuated system with four inputs and six outputs, we need to use an efficient and powerful regulation algorithm that can only work through the mathematical representations of operating the drone system. And we have implemented the design of the basic controllers; It is a PD controller, DSMC with Gao reaching law, and DSMC with power rate reaching law; To choose a suitable controller for the considered system.

2.2 Quad-copter modeling

A system is a set of interrelated objects or phenomena artificially isolated from the outside world; Modeling combines a group of techniques that provide a mathematical representation of the system to be studied.

The synthesis of the control laws of a dynamic system requires a precise modeling of a system so that the model can better predict the behavior of the system to the various excitations (commands, disturbances,..... etc.). Thus, the more detailed it is, the more faithful it is to the system. However, this complicates the study and the synthesis of possible control laws. A compromise must be made by adopting simplifying assumptions to be able to meet the practical constraints.

The quad-rotor is classified in the category of the most complex flying system given the number of physical phenomena that affect its dynamics. In order to design a flight controller, one must first deeply understand the motions of the system and its dynamics. This understanding is necessary not just for controller design, but to ensure that machine simulations will depict behavior as close to reality as possible when the command is applied [1].

The degrees of freedom of the quad-rotor

A quad-rotor is defined in space by six “6 DOF” degrees of freedom (three rotations and three translations); this means that 6 variables are needed to express its position and orientation in space (x, y, z, ϕ, θ and ψ). Where the variables $x, y,$ and z represent the distances of the quad-rotor’s center of mass along the x, y and z -axes respectively from the fixed reference frame. The other three variables are the three Euler angles which represent the quad rotor orientation. ϕ is the angle about the x -axis and is called roll angle, θ is the angle about the y -axis and is called pitch angle, and ψ is the angle about the z -axis and is called yaw angle. Figure 2.1 explains the Euler angles of a quad-rotor. The roll and pitch angles are referred to as the attitudes of the quad-rotor while the yaw angle is called the heading of the quad-rotor. The quad-rotor distance from the ground is called the quad-rotor altitude [19].

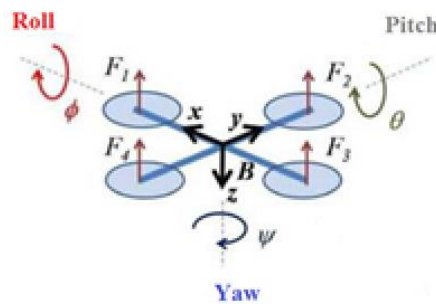


Figure 2. 1. Six degrees of freedom of the quad-rotor

2.3 Quad-copter movements

To achieve the six movements of the quad-rotor we only have four actuators at our disposal, therefore the movements of the device are coupled, which means that we cannot perform one of the movements without involving others. For example, by reducing the speed of the right rotor, the quad-copter tilts to that side and the balance between the rotors which rotate clockwise, and the rotors which rotate counterclockwise is disturbed, which involves two rotational movements called roll and yaw. The roll rotational movement involves a translational movement on the y -axis. This feature that allows the quad-rotor to be controlled over six degrees of freedom with only four actuators. Thus the quad-copter has the following six movements: vertical movement, roll rotation, pitch rotation, yaw rotation translations on the x -axis, and translations on y -axis [20].

2.3.1 Vertical movement

This is provoked by increasing or decreasing all the propeller speeds by the same rate simultaneously. If the quad-copter stays balanced in the horizontal position, this means that the thrust of the quad-copter is equal to the force of gravity. Figure 2.2 demonstrates the vertical translation movement.

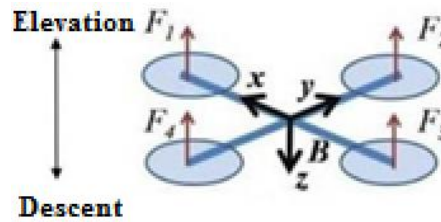


Figure 2. 2. Vertical translation movement

2.3.2 Rotation around the x -axis (Roll)

This movement is provoked by increasing (or decreasing) the speed of the two left (or right) propellers while decreasing (or increasing) the speed of the opposing propellers. It leads to a torque with respect to the x -Axis and make the quad-copter rotate about this axis.

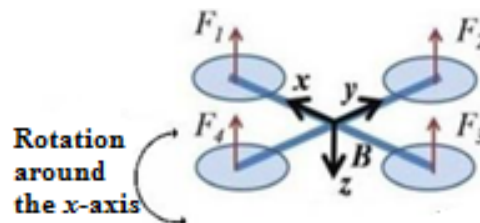


Figure 2. 3. Roll movement

2.3.3 Rotation around y -axis (Pitch)

This movement is provoked by increasing (or decreasing) the speed of the two forward (or backward) propellers while decreasing (or increasing) the speed of the two opposite propellers. It results in a torque with respect to the y -axis and makes the quad-copter rotate about this axis.

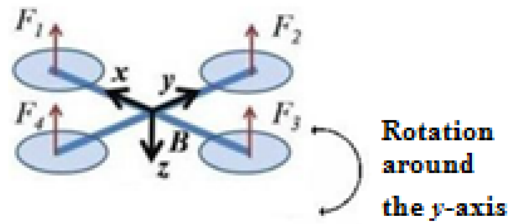


Figure 2. 4. Pitch movement

2.3.4 Rotation around the z -axis (Yaw movement)

This movement is provoked by increasing (or decreasing) the speed of one cross propellers pair clockwise (or counterclockwise) while the other cross propellers pair is decreasing (or increasing). It results in torque with respect to the z -axis and makes the quad-copter rotate around this axis.

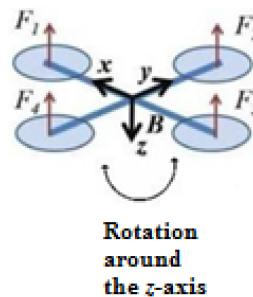


Figure 2. 5. Yaw movement

2.3.5 Translations on the x -axis

To perform a translation on the x -axis, a rotation must be made around the y -axis. This happens if the thrust forces of the two propellers of one side (right or left) are greater or less than the propellers of the other side. That is, rotate the pitch to achieve the withdrawal on the x -axis

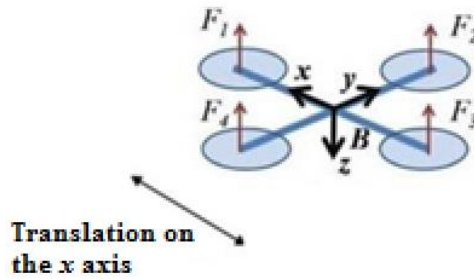


Figure 2. 6. Translation on the X-axis

2.3.6 Translations on the y-axis

To perform a translation on the y-axis, a rotation must be made about the x-axis. This occurs if the thrust forces of the two forward (or backward) propellers are greater or less than the two opposite propellers. That is, rotate the roll to achieve the pull back on the x-axis.

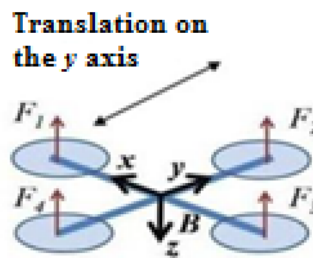


Figure 2. 7. Translation on the Y-axis

2.4 Reference frames

A quad-rotor requires frames to describe its motion in space, Figure 2.8. These frames are:

2.4.1 The inertial frame

It is denoted $R_0(O_0, X_0, Y_0, Z_0)$; it is a reference frame of origin O_0 and axes X_0 , Y_0 and Z_0 linked to the earth, assumed to be immobile.

2.4.2 The body frame (mobile)

It is denoted $R_1(O_1, X_1, Y_1, Z_1)$; It is an origin frame O_1 , which coincides with the center of gravity of the quad-rotor, and axes X_1 , Y_1 and Z_1 . This reference can be obtained by performing three successive rotations defined according to the Z-Y-X convention of Tait-

Bryan, which is the most used in aeronautics, from the reference $R_0 (O_0, X_0, Y_0, Z_0)$. Then a vector translation $(x; y; z)$ from point O_0 along the axes (X_0, Y_0, Z_0) .

We can therefore deduce the parameters that allow us to describe the quad-rotor movement: $(x, y, z, \varphi, \theta, \psi, v_x, v_y, v_z, p, q, r)$

Or:

x (m): the coordinate of point O_I (center of gravity of the quad-rotor) along the X_0 axis.

y (m): the coordinate of point O_I (center of gravity of the quad-rotor) along the Y_0 axis.

z (m): the coordinate of point O_I (center of gravity of the quad-rotor) along the Z_0 axis.

φ (rad): the roll angle. Rotation around the X_I axis $(-\frac{\pi}{2} < \varphi < \frac{\pi}{2})$.

θ (rad): the pitch angle. Rotation around the Y' axis $0 < \theta < \frac{\pi}{2}$.

ψ (rad): the yaw angle. Rotation around the Z_0 axis $(-\pi < \psi < \pi)$.

v_x (m/s): the linear velocity of point O_I along the X_0 axis.

v_y (m/s): the linear velocity of point O_I along the Y_0 axis.

v_z (m/s): the linear velocity of point O_I along the Z_0 axis.

p (rad/s): the angular rate of rotation around the X_I axis.

q (rad/s): the angular rate of rotation around the Y_I axis.

r (rad/s): the angular rate of rotation around the Z_I axis [1].

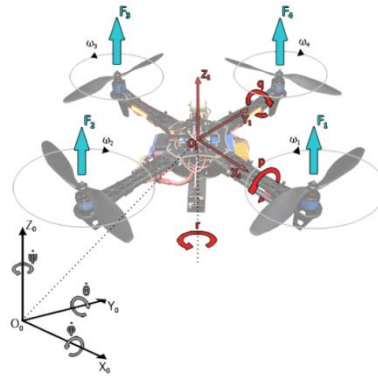


Figure 2. 8. The coordinate frames of the quad-rotor

2.5 Rotation matrix

It is considered that the centers O_0 and O_1 of the two frames coincide, which means that frame R_1 only makes rotations with respect to frame R_0 . Three independent parameters, φ , θ , and ψ , are necessary to completely describe the attitude of the frame R_1 with respect to that of R_0 . The passage from the first marker to the second will be done by three successive rotations following Figure 2.9.

The total rotation matrix that allows us to pass from frame R_1 to frame R_0 is obtained by multiplying three rotation matrices that explained in Appendix A [1]:

$$Rot = R_\psi \times R_\theta \times R_\varphi$$

$$Rot = \begin{bmatrix} \cos(\psi) & -\sin(\psi) & 0 \\ \sin(\psi) & \cos(\psi) & 0 \\ 0 & 0 & 1 \end{bmatrix} \cdot \begin{bmatrix} \cos(\theta) & 0 & \sin(\theta) \\ 0 & 1 & 0 \\ -\sin(\theta) & 0 & \cos(\theta) \end{bmatrix} \cdot \begin{bmatrix} 1 & 0 & 0 \\ 0 & \cos(\varphi) & -\sin(\varphi) \\ 0 & \sin(\varphi) & \cos(\varphi) \end{bmatrix} \quad (2.1)$$

$$Rot = \begin{bmatrix} c(\psi) \cdot c(\theta) & s(\varphi) \cdot s(\theta) \cdot c(\psi) - s(\psi) \cdot c(\varphi) & c(\varphi) \cdot s(\theta) \cdot c(\psi) + s(\psi) \cdot s(\varphi) \\ s(\psi) \cdot c(\theta) & s(\varphi) \cdot s(\theta) \cdot s(\psi) + c(\psi) \cdot c(\theta) & c(\varphi) \cdot s(\theta) \cdot s(\psi) - s(\varphi) \cdot c(\psi) \\ -s(\theta) & s(\varphi) \cdot c(\theta) & c(\varphi) \cdot c(\theta) \end{bmatrix}$$

With: $c = \cos$ $s = \sin$

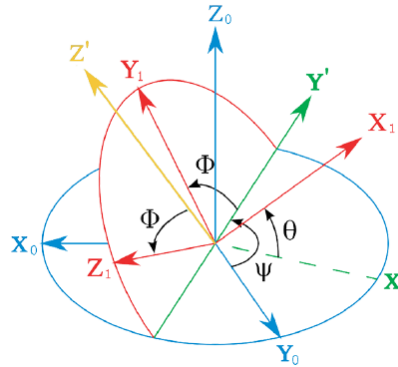


Figure 2. 9. Passage of the marker R0 to the marker R1

2.6 Dynamic model

In what follows, we adopt some simplifying assumptions:

- The structure of the quad-copter is assumed to be rigid and symmetrical.
- The inertia matrix I is assumed to be constant (there is no change in weight).
- The lift and drag forces are assumed to be proportional to the square of the angular speed of the rotors.
- The reference linked to the body of the quad-rotor is assumed to coincide with its center of gravity [21], [22].

Translation dynamics

Through Appendix B, we get, after simplification, the following system of differential equations [1]:

$$\begin{cases} \ddot{x} = \frac{T}{m}(c(\varphi).s(\theta).c(\psi) + s(\varphi).s(\psi)) \\ \ddot{y} = \frac{T}{m}(c(\varphi).s(\theta).s(\psi) - s(\varphi).c(\psi)) \\ \ddot{z} = \frac{T}{m}(c(\varphi).c(\theta)) - g \end{cases} \quad (2. 2)$$

Rotational dynamics

Through Appendix B, we get, after simplification, the following system of differential equations [1]:

$$\begin{cases} \dot{p} = \left(\frac{I_y - I_z}{I_x}\right)qr + \frac{\tau_\phi}{I_x} \\ \dot{q} = \left(\frac{I_z - I_x}{I_y}\right)pr + \frac{\tau_\theta}{I_y} \\ \dot{r} = \left(\frac{I_x - I_y}{I_z}\right)pq + \frac{\tau_\psi}{I_z} \end{cases} \quad (2.3)$$

2.6.1 Relationship between Euler angles and angular velocities

If a solid rotates at a constant speed, its angular velocity Ω is constant; on the other hand, the variations of the Euler angles will be variable because they depend on the instantaneous angles between the axes of the two reference frames. The sequence of Euler angles is obtained from three successive rotations: yaw, pitch, and roll. Variation ψ requires two rotations, θ requires rotation and ϕ does not require any rotation [23]:

$$\Omega = R_\phi \cdot R_\theta \begin{bmatrix} 0 \\ 0 \\ \dot{\psi} \end{bmatrix} + R_\phi \begin{bmatrix} 0 \\ \dot{\theta} \\ 0 \end{bmatrix} + \begin{bmatrix} \dot{\phi} \\ 0 \\ 0 \end{bmatrix} \quad (2.4)$$

This gives us:

$$\begin{bmatrix} p \\ q \\ r \end{bmatrix} = \begin{bmatrix} 1 & 0 & -\sin(\theta) \\ 0 & \cos(\phi) & \sin(\phi)\cos(\theta) \\ 0 & -\sin(\phi) & \cos(\phi)\cos(\theta) \end{bmatrix} \begin{bmatrix} \dot{\phi} \\ \dot{\theta} \\ \dot{\psi} \end{bmatrix} \quad (2.5)$$

For reasons of simplification and since most of the cases studied in the literature work with a simplified model, it is assumed that the roll and pitch angles are of low amplitude, $|\phi| \leq \frac{\pi}{9}$ and $|\theta| \leq \frac{\pi}{9}$, which allows us to have $\sin(\phi) \approx \phi$, $\sin(\theta) \approx \theta$, $\cos(\phi) \approx 1$ and $\cos(\theta) \approx 1$ and it is also assumed that the angular velocities around the three axes of the quad-copter are small, and therefore the equation (2.5) becomes [1]:

$$\begin{bmatrix} p \\ q \\ r \end{bmatrix} = \begin{bmatrix} \dot{\phi} - \sin(\theta)\dot{\psi} \\ \cos(\phi)\dot{\theta} + \sin(\phi)\cos(\theta)\dot{\psi} \\ -\sin(\phi)\dot{\theta} + \cos(\phi)\cos(\theta)\dot{\psi} \end{bmatrix} \approx \begin{bmatrix} \dot{\phi} \\ \dot{\theta} \\ \dot{\psi} \end{bmatrix} \quad (2.6)$$

And the equation (2.3) becomes:

$$\begin{cases} \ddot{\varphi} = \left(\frac{I_y - I_z}{I_x}\right) \dot{\theta}\dot{\psi} + \frac{\tau_{\varphi}}{I_x} \\ \ddot{\theta} = \left(\frac{I_z - I_x}{I_y}\right) \dot{\varphi}\dot{\psi} + \frac{\tau_{\theta}}{I_y} \\ \ddot{\psi} = \left(\frac{I_x - I_y}{I_z}\right) \dot{\varphi}\dot{\theta} + \frac{\tau_{\psi}}{I_z} \end{cases} \quad (2.7)$$

2.6.2 Rotor dynamics

Quad-rotors are usually equipped with brushless or BLDC motors, which are brushless motors and therefore require each phase to be powered by an external power source during the correct rotation cycle. To do this, a power circuit called ESC (Electronic Speed Controller) is used to perform the functions of the inverter and the control circuit. The pair: BLDC motor and the ESC are powered by DC voltage and therefore behave like a DC motor, hence the name "Brushless DC".

In the following, we consider the BLDC motor and ESC pair to be equivalent to a brushed DC motor, and we denote V_{EQ} as the effective voltage applied by the ESC across the BLDC motor terminals, Figure 2.10 [1].

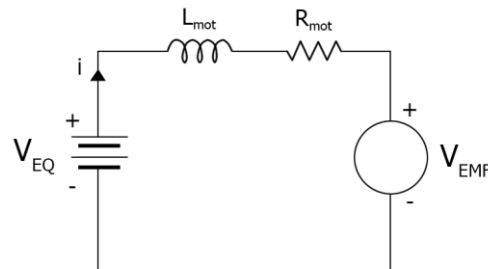


Figure 2. 10. Equivalent electrical circuit

Using the mesh law, we get:

$$V_{EQ} = R_{mot}i + L_{mot} \cdot \frac{di}{dt} + V_{EMF} \quad (2.8)$$

With:

$V_{EMF} = K_e \cdot \omega$ is the back electromotive force, I_r

Ω is the angular speed of the rotor,

K_e is the electrical constant of the motor,

L_{mot} is the equivalent inductance of the motor,

R_{mot} is the equivalent resistance of the motor.

For small-size motors, like those used for quad-copters, the inductance is very small, and therefore the electrical part is much faster than the mechanical part. Equation (2.8) becomes:

$$V_{EQ} = R_{mot}i + K_e \cdot \omega \quad (2.9)$$

For the mechanical part presented in Figure 2.11, we use Newton's second law is used to extract the equation (2.10).

$$I_r \dot{\omega} = \Gamma_e + \Gamma_r \quad (2.10)$$

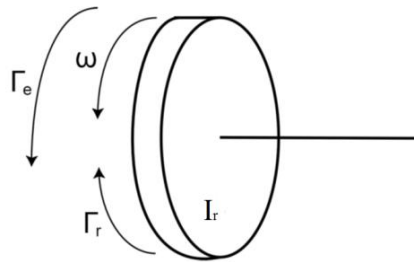


Figure 2. 11. Mechanical part of the motor

With:

$\Gamma_e = K_e \cdot i$ represents the electric torque provided by the motor.

$\Gamma_r = - f_r \cdot \omega$ represents the torque due to air friction.

Equation (2.10) then becomes:

$$I_r \dot{\omega} = K_e \cdot i - f_r \cdot \omega \quad (2.11)$$

Using Laplace transform of equations (2.9) and (2.11) and simplifying we get:

$$\frac{\omega(s)}{V_{EQ}(s)} = \frac{1}{\frac{R_{mot} \cdot I_r}{K_e} \cdot s + f_r + K_e} \quad (2.12)$$

The equivalent voltage V_{EQ} is the voltage generated by the ESC according to the control signal u_{PWM} which represents the width of the PWM signal (Pulse Width Modulation) received at the input. The relationship between V_{EQ} and u_{PWM} is given as follow:

$$V_{EQ} = u_{PWM} V_B \quad (2.13)$$

With: V_B is the voltage available at the input.

The expression of u_{PWM} is given by:

P is the pulse width at time t .

P_{max} is the maximum width of the pulse.

P_{min} is the minimum pulse width.

Equation (2.12) finally becomes:

$$\frac{\omega(s)}{u_{PWM}(s)} = \frac{K}{T \cdot s + 1} \quad (2.14)$$

With:

$$K = \frac{V_B}{f_r + K_e} \quad (2.15)$$

and

$$T = \frac{R_{mot} \cdot I_r}{K_e (f_r + K_e)} \quad (2.16)$$

Due to the relatively small size of the motors, we neglect what follows their dynamics compared to that of the quad-rotor. We finally get:

$$\frac{\omega}{u_{PWM}} = K \quad (2.17)$$

2.7 State model

To put the quad-rotor equations in state space form, we choose as state vector

$$X = [x \ \dot{x} \ y \ \dot{y} \ z \ \dot{z} \ \varphi \ \dot{\varphi} \ \theta \ \dot{\theta} \ \psi \ \dot{\psi}]^T \quad (2.18)$$

$$X = [x_1 \ x_2 \ x_3 \ x_4 \ x_5 \ x_6 \ x_7 \ x_8 \ x_9 \ x_{10} \ x_{11} \ x_{12}]^T \quad (2.19)$$

and the commands [1]:

$$\begin{cases} U_1 = T = b \cdot (\omega_1^2 + \omega_2^2 + \omega_3^2 + \omega_4^2) \\ U_2 = \tau_\varphi = l \cdot b (\omega_4^2 - \omega_2^2) \\ U_3 = \tau_\theta = l \cdot b (\omega_3^2 - \omega_1^2) \\ U_4 = \tau_\psi = k \cdot (-\omega_1^2 + \omega_2^2 - \omega_3^2 + \omega_4^2) \end{cases} \quad (2.20)$$

The resulting state representation is as follows:

$$\begin{cases} \dot{x}_1 = x_2 \\ \dot{x}_2 = \frac{U_1}{m} (c_{x7} s_{x8} c_{x9} + s_{x7} s_{x9}) \\ \dot{x}_3 = x_4 \\ \dot{x}_4 = \frac{U_1}{m} (c_{x7} s_{x8} s_{x9} - s_{x7} c_{x9}) \\ \dot{x}_5 = x_6 \\ \dot{x}_6 = \frac{U_1}{m} (c_{x7} c_{x8}) - g \\ \dot{x}_7 = x_8 \\ \dot{x}_8 = \left(\frac{I_y - I_z}{I_x} \right) x_{11} x_{12} + \frac{U_2}{I_x} \\ \dot{x}_9 = x_{10} \\ \dot{x}_{10} = \left(\frac{I_z - I_x}{I_y} \right) x_{10} x_{12} + \frac{U_3}{I_y} \\ \dot{x}_{11} = x_{12} \\ \dot{x}_{12} = \left(\frac{I_x - I_y}{I_z} \right) x_{10} x_{11} + \frac{U_4}{I_z} \end{cases} \quad (2.21)$$

State model in discrete time:

$$\left\{ \begin{array}{l} x_1[k+1] = x_2[k] \\ x_2[k+1] = \frac{U_1[k]}{m} (c_{x7[k]} s_{x8[k]} c_{x9[k]} + s_{x7[k]} s_{x9[k]}) \\ x_3[k+1] = x_4[k] \\ x_4[k+1] = \frac{U_1[k]}{m} (c_{x7[k]} s_{x8[k]} s_{x9[k]} - s_{x7[k]} c_{x9[k]}) \\ x_5[k+1] = x_6[k] \\ x_6[k+1] = \frac{U_1[k]}{m} (c_{x7[k]} c_{x8[k]}) - g \\ x_7[k+1] = x_8[k] \\ x_8[k+1] = \left(\frac{I_y - I_z}{I_x} \right) x_{11}[k] x_{12}[k] + \frac{U_2[k]}{I_x} \\ x_9[k+1] = x_{10}[k] \\ x_{10}[k+1] = \left(\frac{I_z - I_x}{I_y} \right) x_{10}[k] x_{12}[k] + \frac{U_3[k]}{I_y} \\ x_{11}[k+1] = x_{12}[k] \\ x_{12}[k+1] = \left(\frac{I_x - I_y}{I_z} \right) x_{10}[k] x_{11}[k] + \frac{U_4[k]}{I_z} \end{array} \right. \quad (2.22)$$

As can be seen, the system is naturally divided into two coupled subsystems: a translational subsystem and a rotational subsystem.

$$\begin{bmatrix} x_1[k+1] \\ x_3[k+1] \\ x_5[k+1] \\ x_7[k+1] \\ x_9[k+1] \\ x_{11}[k+1] \end{bmatrix} = \begin{bmatrix} 0 \\ 0 \\ -g \\ \left(\frac{I_y - I_z}{I_x} \right) x_{11}[k] x_{12}[k] \\ \left(\frac{I_z - I_x}{I_y} \right) x_{10}[k] x_{12}[k] \\ \left(\frac{I_x - I_y}{I_z} \right) x_{10}[k] x_{11}[k] \end{bmatrix} + \begin{bmatrix} \frac{U_1[k]}{m} (c_{x7[k]} s_{x8[k]} c_{x9[k]} + s_{x7[k]} s_{x9[k]}) \\ \frac{U_1[k]}{m} (c_{x7[k]} s_{x8[k]} s_{x9[k]} - s_{x7[k]} c_{x9[k]}) \\ \frac{U_1[k]}{m} (c_{x7[k]} c_{x8[k]}) \\ \frac{U_2[k]}{I_x} \\ \frac{U_3[k]}{I_y} \\ \frac{U_4[k]}{I_z} \end{bmatrix} \quad (2.23)$$

2.8 Discrete Time quad-rotor's model

The dynamic model can be written in the following compact:

$$\dot{x}(t) = \begin{cases} x_{2i-1}(t) = x_{2i}(t), & i = 1, 2, \dots, 6 \\ x_{2i}(t) = f_i(x(t)) + \Delta f_i(x(t)) + (g_i(x(t)) + \Delta g_i(x(t))) u(t) + \omega_i(t) \end{cases} \quad (2.24)$$

As a result of forward Euler discretization, we obtain the following discrete system for equation (2.25):

$$x[k] = \begin{cases} x_{2i-1}[k+1] = x_{2i-1}[k] + hx_{2i}[k] & i = 1, 2, \dots, 6 \\ x_{2i}[k] = x_{2i}[k] + h(f_i(x[k]) + \Delta f_i(x[k]) + \\ (g_i(x[k]) + \Delta g_i(x[k]))u[k] + \omega_i[k] \end{cases} \quad (2.25)$$

Where k represents the k -th sampling time, h represents sampling time, $f_i(x[k])$ and $g_i(x[k])$. $\Delta f_i(\cdot)$, $\Delta g_i(\cdot)$, denote the bounded unknown parametric uncertainties, $\omega_i[k]$ is the bounded external disturbance, where: $\Delta f_i(\cdot) \leq \Delta f_{i_{max}}$, $\Delta g_i(\cdot) \leq \Delta g_{i_{max}}$ and $\omega_i[k] \leq \omega_{i_{max}}$.

Dynamic system equation (2. 26) is written as follows:

$$\begin{cases} x_{2i-1}[k+1] = x_{2i-1}[k] + hx_{2i}[k], & i = 1, 2, \dots, 6 \\ x_{2i}[k+1] = x_{2i}[k] + h(f_i(x[k]) + g_i(x[k])u[k] + d[k] \end{cases} \quad (2. 26)$$

Where

$$d[k] = h(\Delta f_i(x[k]) + \Delta g_i(x[k])u[k]) + \omega_i[k] \quad (2.27)$$

Let $u[k] = [u_1[k], u_2[k], u_3[k], u_4[k]]^T$ being the control input. Objective is to create non-linear control laws to track a quad-rotor along a desired trajectory $\{x_d, y_d, z_d, \psi_d\}$. Next, we assume that there are no disturbances ($d[k] = 0$) and controllers are unknown of it [24].

2.9 Controller design

Many controllers are designed to control quad-copter in linear or nonlinear case. The PD controller is a linear controller and the DSMC is a nonlinear controller. Figure 2.12 shows the main structure (or scheme) used for designing a controller.

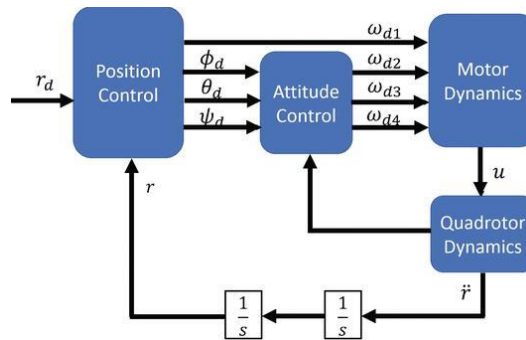


Figure 2. 12. Design controller scheme

2.9.1 Design of PD controller

The PD controller also includes two loops, an outer loop and an inner loop. The outer ring is the position controller, and the inner loop is the attitude controller. In this controller, we are using the same dynamic model as the designed controller given in Figure 2.12.

In order to control the position of the drone, it is necessary to make two control loops: a low-level loop, which will make it possible to control the attitude of the quad-copter (φ, θ, ψ), and a high-level loop, which will control its position (x, y, z). Since a quad-copter is an under-actuated system, the x and y position control loops drive the φ and θ position control loops. Thus, the high-level control will give us the desired Euler angles which will make it possible to correct the position of the drone, and the low-level control will control the rotation speeds of the rotors so that the Euler angles precisely follow the angles desired. The control loops in z and in ψ act directly on the speed rotation of the motors[25].

The corresponding control inputs are given in below.

$$\begin{cases} U_1[k] = \frac{m}{U_z[k]} [g + k_{pz} (z_d[k] - z[k]) + k_{dz} (z_d[k+1] - z[k+1])] \\ U_2[k] = k_{p\varphi} (\varphi_d[k] - \varphi[k]) + k_{d\varphi} (\varphi_d[k+1] - \varphi[k+1]) \\ U_3[k] = k_{p\theta} (\theta_d[k] - \theta[k]) + k_{d\theta} (\theta_d[k+1] - \theta[k+1]) \\ U_4[k] = k_{p\psi} (\psi_d[k] - \psi[k]) + k_{d\psi} (\psi_d[k+1] - \psi[k+1]) \end{cases} \quad (2.28)$$

We then choose the desired Euler angles according to the position errors are:

$$\begin{cases} \varphi_d = \text{asin}(\frac{U_x[k] s_\psi - U_y[k] c_\psi}{c_{\varphi_d}}) \\ \theta_d = \text{asin}(\frac{U_x[k] c_\psi + U_y[k] s_\psi}{c_{\varphi_d}}) \end{cases} \quad (2.29)$$

with:

$$\begin{cases} U_x[k] = \frac{m}{U_1[k]} [k_{px} (x_d[k] - x[k]) + k_{dx} (\dot{x}_d - \dot{x})] \\ U_y[k] = \frac{m}{U_1[k]} [k_{py} (y_d[k] - y[k]) + k_{dy} (y_d[k+1] - y[k+1])] \end{cases} \quad (2.30)$$

2.9.2 Design of DSMC with Gao's reaching law

SMC law attempts to constrain the trajectory of the system state (2.26), allowing the system to maintain itself on a sliding surface regardless of uncertainty. Let's choose a second-order Slotine surface as follows:

The real commands $u[k] = [u_1[k], u_2[k], u_3[k], u_4[k]]^T$ is:

$$U_1[k] = m \sqrt{(v_x[k])^2 + (v_y[k])^2 + (v_z[k] + g)^2} \quad (2.31)$$

$$\begin{cases} U_2[k] = I_x v_\phi[k] - (I_y - I_z) x_{11}[k] x_{12}[k] \\ U_3[k] = I_y v_\theta[k] - (I_z - I_x) x_{10}[k] x_{12}[k] \\ U_4[k] = I_z v_\psi[k] - (I_x - I_y) x_{10}[k] x_{11}[k] \end{cases} \quad (2.32)$$

The desired roll angles φ_d and pitch angles θ_d are generated from:

$$\begin{cases} m(v_x[k]c_\psi + v_y[k]s_\psi) = s_\theta U_1[k] \\ m(v_x[k]s_\psi - v_y[k]c_\psi) = s_\phi c_\theta U_1[k] \\ m(v_z[k] + g) = c_\phi c_\theta U_1[k] \end{cases} \quad (2.33)$$

we draw from the equation (2.33).

$$\begin{cases} \varphi_d = \arctan\left(\frac{v_x[k]s_{\psi_d} - v_y[k]c_{\psi_d}}{v_z[k] + g}\right) \\ \theta_d = \arctan\left(\frac{v_x[k]c_{\psi_d} + v_y[k]s_{\psi_d}}{\sqrt{(v_x[k]s_{\psi_d} - v_y[k]c_{\psi_d})^2 + (v_z[k] + g)^2}}\right) \end{cases} \quad (2.34)$$

2.9.3 Design of DSMC with Power rate reaching law

In the Power rate reaching law, we will follow the same steps in Gao's reaching law, but we will change the equation of the Gao access dynamics of the sliding surface that we find in Appendix C, and replace it with the following formulation.

$$s_i[k + 1] = (1 - h\sigma_i)s_i[k] - h\mu_i |s_i[k]|^\eta \text{sign}(s_i[k]), \quad i = 1, 2, \dots, 6 \quad (2.35)$$

Commands virtual becomes as follows:

$$v_i[k] = \sigma_i s_i[k] + \mu_i |s_i[k]|^\eta \text{sign}(s_i[k]) + \lambda_i e_{2i-1}[k + 1] + \tau_{2i}[k + 1], \quad i = 1, 2, \dots, 6 \quad (2.36)$$

The real commands $u[k] = [u_1[k], u_2[k], u_3[k], u_4[k]]^T$ is determined from $v_i[k]$.

$$\begin{cases} U_1[k] = m \sqrt{(v_x[k])^2 + (v_y[k])^2 + (v_z[k] + g)^2} \\ U_2[k] = I_x v_\varphi[k] - (I_y - I_z)x_{11}[k] x_{12}[k] \\ U_3[k] = I_y v_\theta[k] - (I_z - I_x)x_{10}[k] x_{12}[k] \\ U_4[k] = I_z v_\psi[k] - (I_x - I_y)x_{10}[k] x_{11}[k] \end{cases} \quad (2.37)$$

2.10 Conclusion

In this chapter, the modeling aspect has been presented. First, the mathematical modeling of the quad-copter is given. Then, the main controllers used for controlling quad-copter have been discussed. The simulation results of quad-copter using the presented models will be shown in the next chapter.



Chapter 03

*Simulation and
conception of a drone*



3.1 Introduction

This chapter concerns simulation, design and implementation of a quad-copter. The realization of the proposed quad-copter is based on the following steps:

First, the simulation results for PD and DSMC controllers will be presented for comparison. Then we go to the practical side, Starting with the hardware components used to build a quad-copter are selected and described in detail. A radio control device for controlling the developed quad-copter is used. The development of the quad-copter is based on different software.

Then, power distribution, component positions and connections across the quad-copter's physical framework are described. Calibration of the quad-copter has been performed to ensure its stability.

Finally, to evaluate the drone performances such as stability, precision and equilibrium several experiments have been realized.

3.2 Part1: Simulation results

In this section, simulation results using Matlab-Simulink are developed to assess the effectiveness of the proposed controllers. The quad-rotor's parameters used in these simulations were obtained from our real quad-rotor platform. The sampling period of the simulation is set to $h = 0.01$ s, and the initial conditions, $x_0 = \text{zeros}(12,1)$, are set to zero in the nominal case. The dynamic controllers' parameters that stabilize the quad-rotor are listed in Table D. 1, Table D. 2, Table D. 3, Table D. 4, and Table D. 5. Appendix D.

The reference trajectory (an 8-shaped inclined trajectory) is designed as follows:

$$x_d = 4 \cos\left(\frac{\pi}{40} \cdot t\right) \text{ m} \quad (3.1)$$

$$y_d = 4 \sin\left(\frac{\pi}{20} \cdot t\right) \text{ m} \quad (3.2)$$

$$z_d = 4 - 2 \cos\left(\frac{\pi}{40} \cdot t\right) \text{ m} \quad (3.3)$$

$$\psi_d = \frac{\pi}{3} \cdot (10 t^3 - 15 t^4 + 6 t^5) \text{ rad} \quad (3.4)$$

3.2.1 Nominal conditions

In this case, without considering any disturbances or parametric uncertainties, simulations of the closed-loop system with three different controllers are carried out to track an 8-shaped

inclined trajectory. Figure 3.1, Figure 3.2 and Figure 3.3 illustrate the tracking performance of the controllers.

As shown in Figures 3.1(a)-3.1(b)-3.1(c) and 3.1(d), all controllers achieve successful tracking. In contrast, Gao’s reaching law and power rate reaching law display a faster response time than PD.

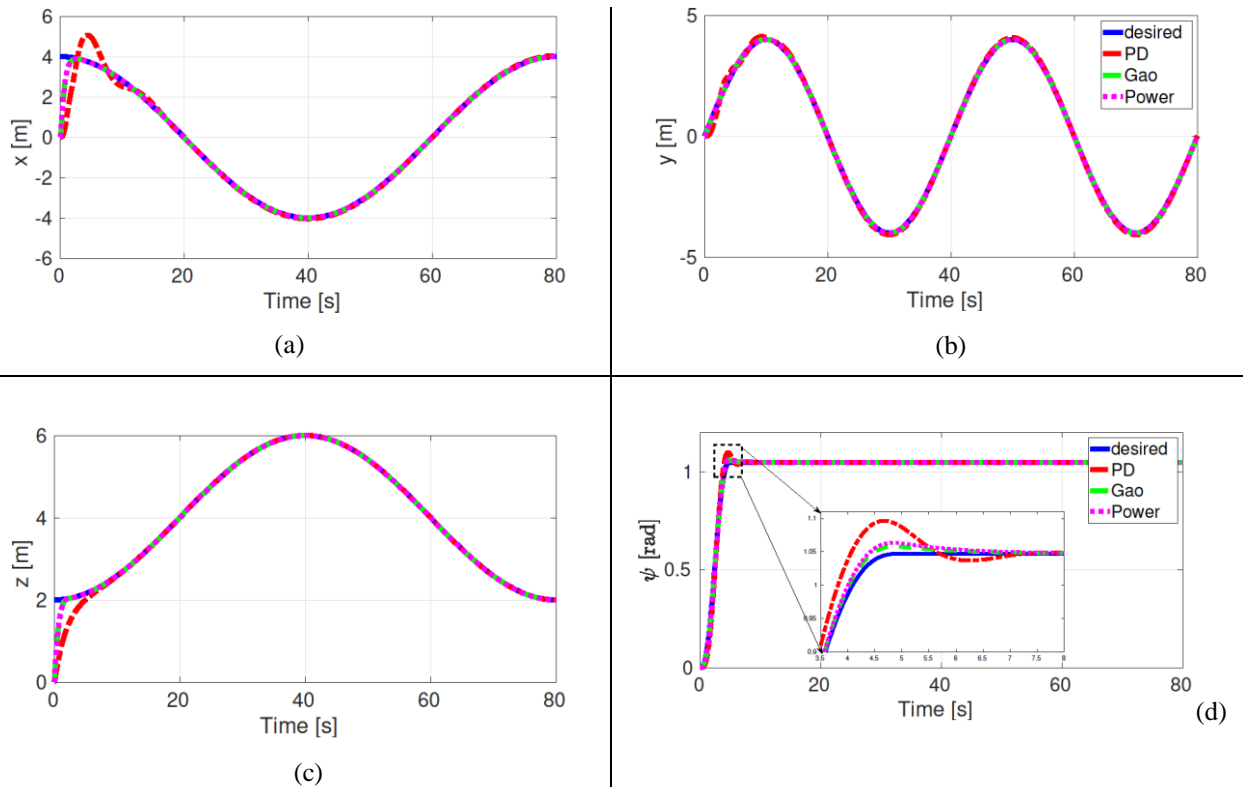


Figure 3. 1.(a)-(b)-(c) Evaluate the position according to the three axes X, Y, Z, (d) Evaluation of the yaw angle .

In fig 3.2(a) and 3.2(b), we note that the error of the angles in Gao’s reaching law and power rate reaching law are almost equal; On the other hand, PD has oscillations that end at

$$T = 7s \text{ for } \varphi_e, \text{ and at } T = 20s \text{ for } \theta_e.$$

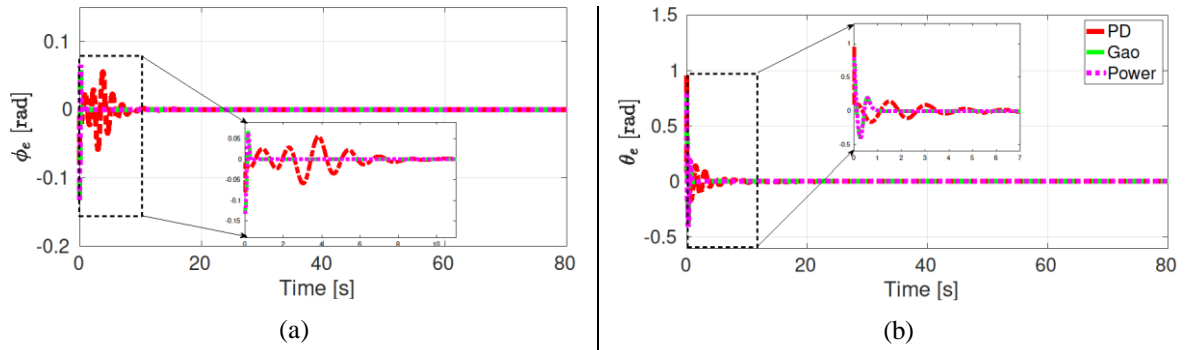


Figure 3. 2 (a),(b) Evaluation the error of the roll and pitch angles.

In Figure 3.3(a), we note that the thrust force U_1 in Gao’s reaching law and power rate reaching law are almost equal, and they start with a high value, unlike in PD it starts with a small value. Same thing in Figure 3.3(c), it noted that the torque U_3 in Gao’s reaching law and power are almost equal, and they start with a high value, unlike PD it starts with a small value.

In Figure 3.3(b) and Figure 3.3(d), we note that the torques U_2 and U_4 in Gao’s reaching law, power rate reaching law, and PD are roughly equal.

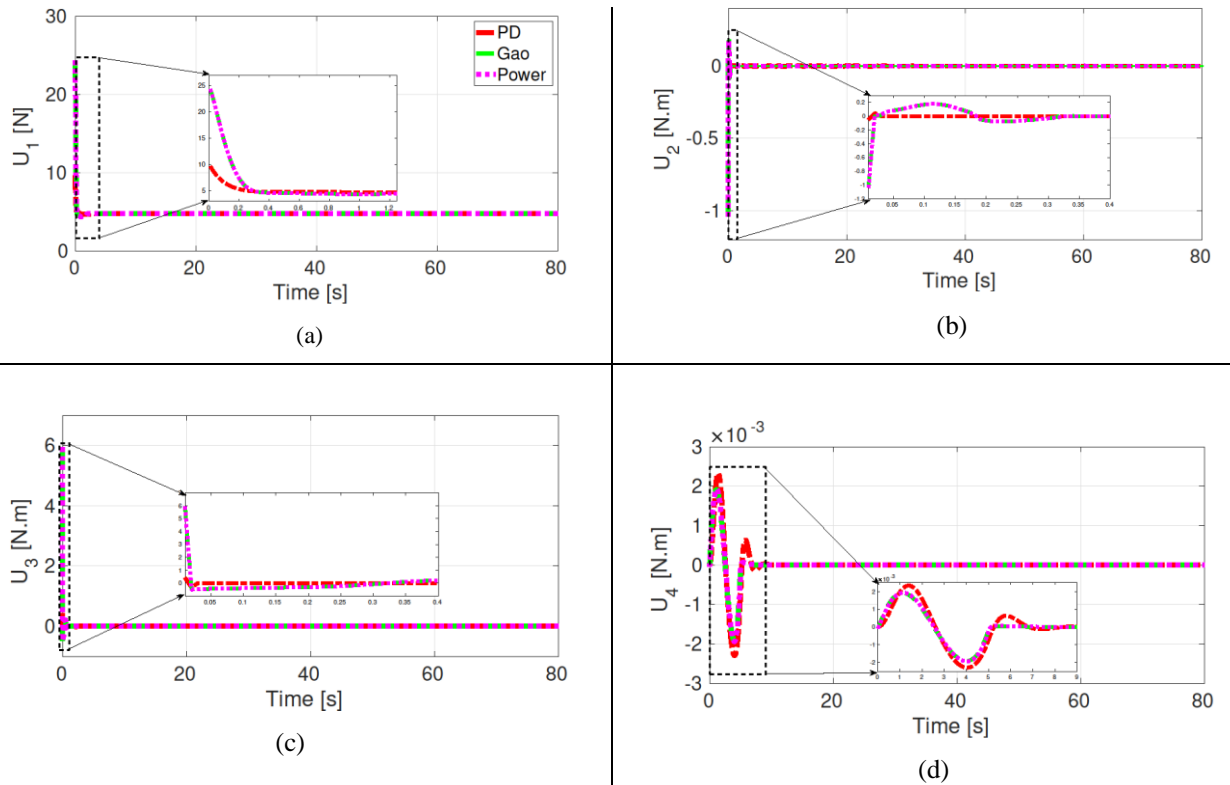


Figure 3. 3. Evaluate of the controls U_1, U_2, U_3 and U_4 .

3.2.2 The controllers' assessment in the presence of model mismatch and perturbations

We applied a disturbance d in the interval $t \in]10; 15]$ for U_1 .

Where:

$$d = 3\sin(t) \cdot e^{-t} \quad (3.7)$$

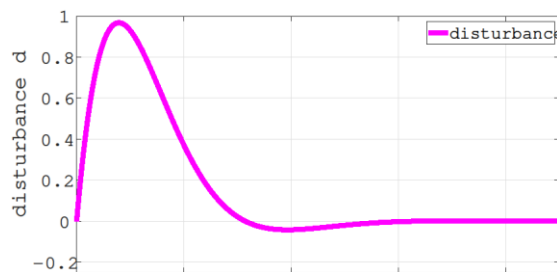


Figure 3. 4. Disturbance d

As we applied a disturbance dx in the interval $t \in]20; 25[$ for U_2 , U_3 and U_4 .

Where:

$$dx = \sin\left(\frac{t}{3}\right) \cdot e^{-t} \quad (3.8)$$

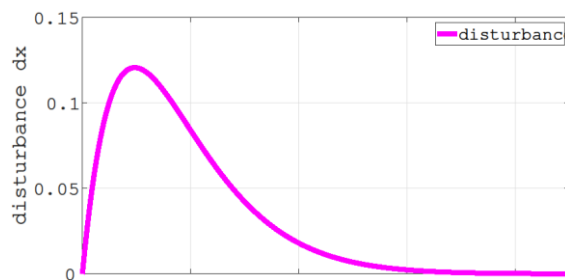


Figure 3. 5. Disturbance dx

Since the model parameters m , I_x , I_y and I_z are variants, 20% variations of these model parameters are assumed as follows in interval $t \in]20; 25[$:

$$m_tilda = (1+0.2) * m \tag{3.9}$$

Where, m_tilda is mismatch mass

$$I_{x_tilda} = (1+0.2) * I_x \tag{3.10}$$

$$I_{y_tilda} = (1+0.2) * I_y \tag{3.11}$$

$$I_{z_tilda} = (1+0.2) * I_z \tag{3.12}$$

Where, I_{x_tilda} , I_{y_tilda} , I_{z_tilda} is mismatch inertial.

The simulation here is performed using disturbances, to track an 8-shaped inclined trajectory under perturbations and parametric uncertainties, and with an initial state different from the equilibrium point. Simulation results, in this case, are shown in Figure.3.6, Figure.3.7 and Figure.3.8.

As shown in Figures 3.6 (a) - 3.6(b) -3.6(c) and 3.6(d), all controllers achieve an oscillation at first, and then tracking becomes successful. Furthermore when disturbance and uncertainty are applied, there are oscillations where Gao’s reaching law and power rate reaching law display a faster response time than PD.

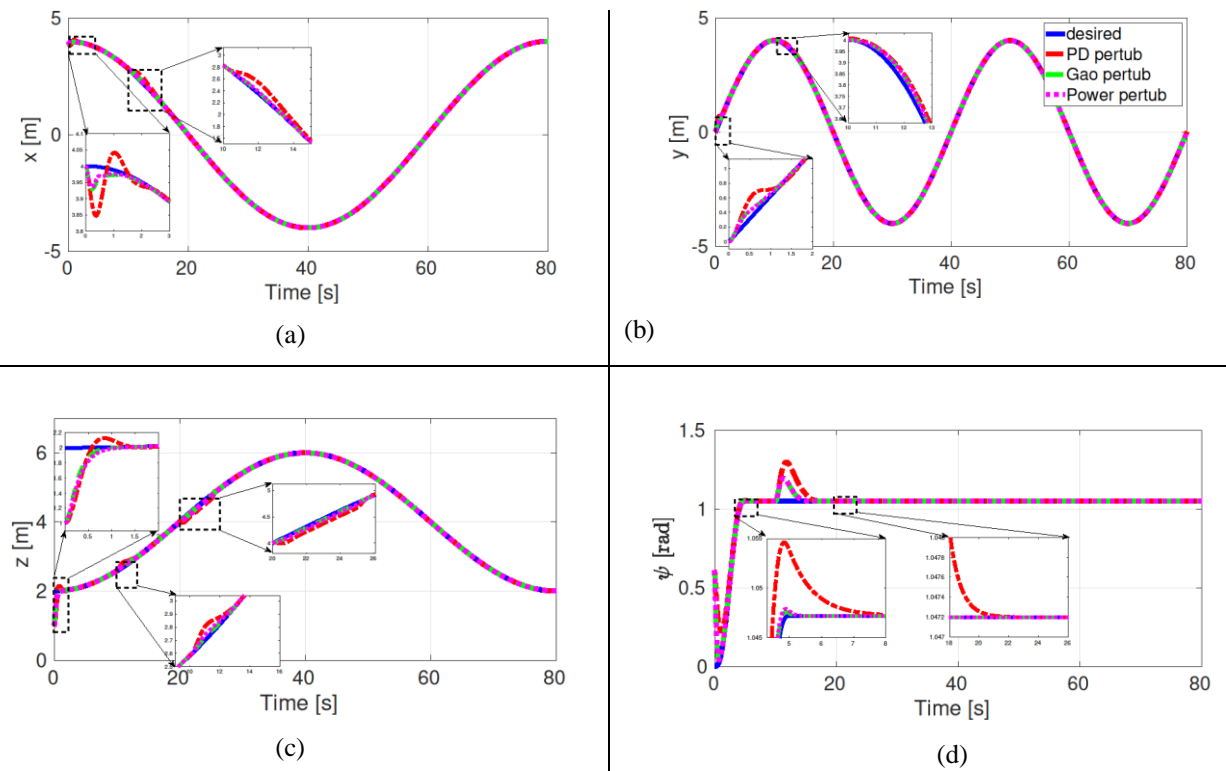


Figure 3. 6. (a)-(b)-(c) Evaluate the position according to the three axes X, Y, Z, (d) Evaluation of the yaw angle of the applied turbulence in interval $t \in]10; 15]$ and $t \in]20; 25]$.

In Figure.3.7 (a) and 3.7 (b) we note that the angles' error of Gao's reaching law, power rate reaching law, and PD are almost equal, however, in uncertainty time, we note that Gao and power are better than PD.

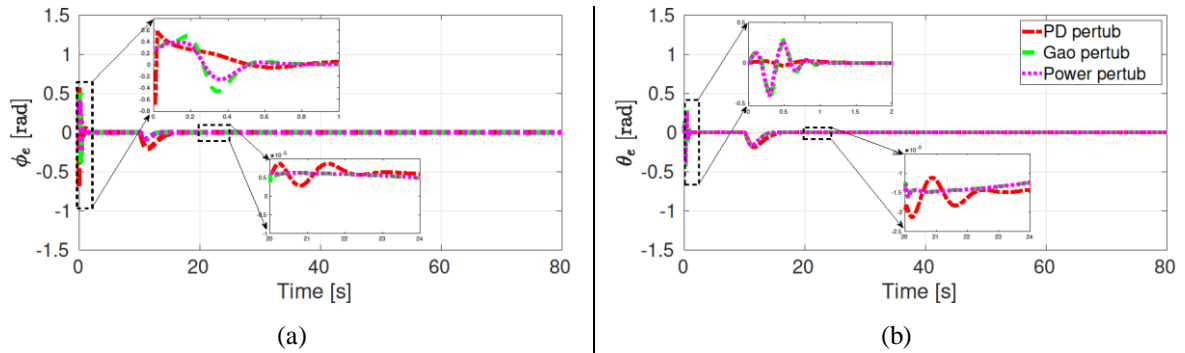


Figure 3.7. (a), (b) Evaluation the error of the roll and pitch angles of the applied turbulence in interval $t \in]10; 15 [$ and $t \in]20; 25 [$.

In Figure.3.8 (a), we notice that the thrust force U_1 in Gao's reaching law starts with a high value compared to the power rate reaching law and PD. In Figure.3.8 (b), we note that the torque U_2 in Gao's reaching law and the power rate reaching law are approximately equal and starts with a small value, unlike PD begins with a high value.

In Figure.3.8 (c) and Figure.3.8 (d), we notice that the torques U_3 and U_4 in Gao's reaching law and power rate reaching law are almost equal with a high value, but in PD has a small value. In all figures we notice that in disturbance Gao's reaching law and force are better than PD.

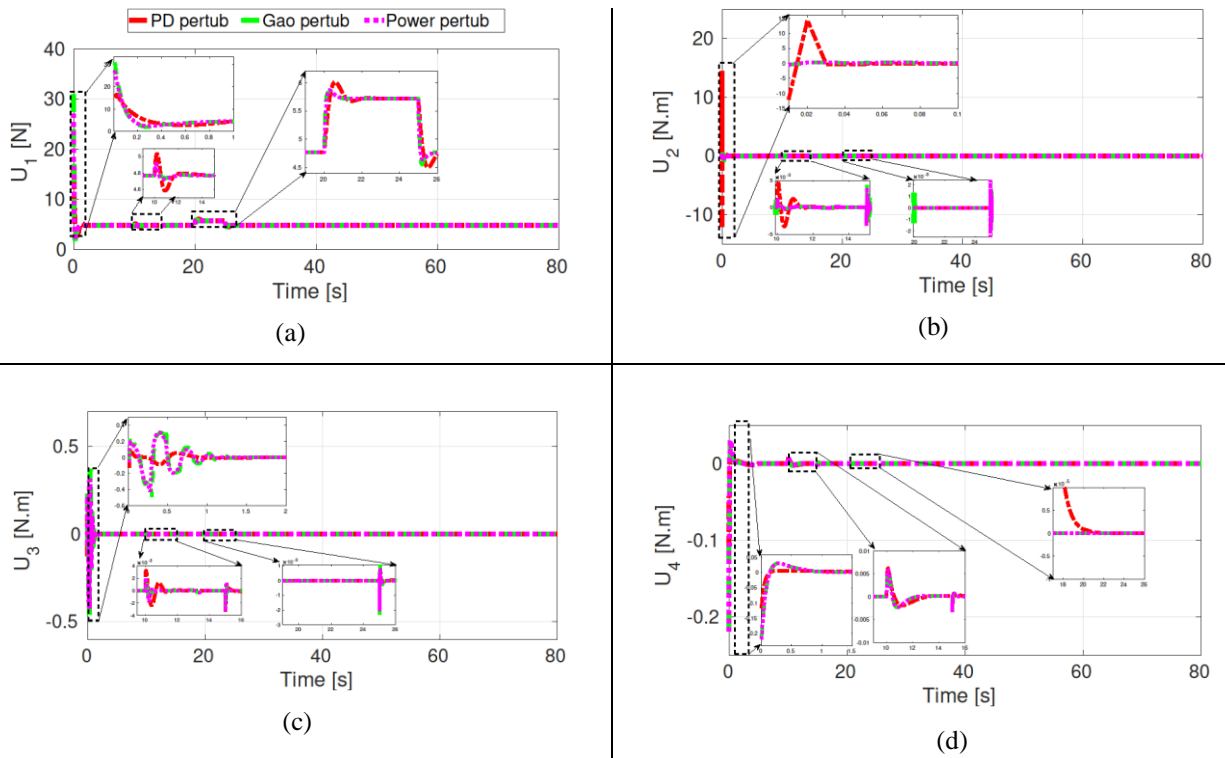


Figure 3. 8. Evaluate of the controls U_1 , U_2 , U_3 and U_4 of the applied turbulence in interval $t \in]10; 15]$ and $t \in]20; 25[$.

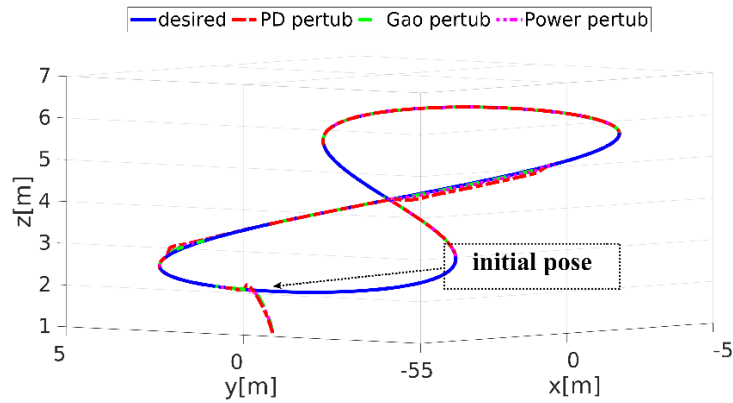


Figure 3. 9. The 3-D traking trajectory

We conclude from the simulation results that the Gao's reaching law and power rate reaching law controllers provide a faster response speed than the PD controller, meaning that the error processing speed was faster than the error processing speed at the PD controller even in the presence of perturbation or uncertainties. But the drawback of Gao's reaching law and power rate reaching law controllers is the need for more control efforts compared to the PD controller, i.e., more power consumption.

3.3 Part 2: Design and conception

3.3.1 Mechanical components

3.3.1.1 Frame

The choice of the frame (or its construction) is the most important step in the realization of a drone. On this frame other components are mounted.

There are several types of propeller drone frames: H shaped frame, X shaped frame, + shaped frame, six-arm frame, eight-arm frame, etc.

Whoever, the type of material used to build the frame represents an important criterion in the design. Each material has advantages and disadvantages. Some materials and their characteristics are given as follow:

- Wood: inexpensive but fragile.
- Aluminum: a light, solid, easy to work with, and inexpensive material.
- Carbon fiber: is undoubtedly the most suitable material for this type of construction due to its strength and lightness, but it is also the most expensive.
- Plastic: the most widely used material because of its diversity, as it combines lightness, rigidity and low cost.

There are also other materials that can be used [19].

3.3.1.2 The propellers

The choice of propellers is very important because we need propellers that are adapted to the type of flight we want to achieve, large propellers (between 9 and 11 inches) ensure a more stable flight and can lift more weight and smaller propellers between 5 and 8 inches requires a lighter structure.

The materials used in the construction of fans are numerous:

- Plastic: The most common material for making fans, making it possible to get solid, inexpensive fans.
- Wood: Wood fans are less common and have interesting properties in terms of durability and hardness, but it is not easy to find this material.

- Carbon fiber: considered as the most reliable but also the most expensive material [19].

3.3.2 Electrical components

3.3.2.1 Brushless motors

Brushless motors are DC motors that do not use commutator brushes because the coils are powered directly and a permanent magnet is placed on the rotor.

Brushless motors have their own KV, which is the number of revolutions per minute that the motor makes for a voltage of 1 volt and is proportional to the input voltage. For example, an 800KV motor with 12V input will run at 9600 rpm. The higher the KV of the engine, the higher its speed and the lower the engine torque. Also, as the value of KV decreases, the engine speed decreases and its torque increases.

Therefore, the choice of motor depends on the KV ratio and takes into account the type of flight and the size of the propellers, for a stable flight you need large propellers and motors with high torque and a small KV ratio, for a “nervous” or fast flight, small propellers and motors are needed It has a high kV ratio [19].

3.3.2.2 Electronic Speed Controller (ESC)

Electronic speed control (ESC) is small electronic cards that control the speed of brushless motors. They accept as input a supply voltage (generally 12V) and a control voltage sent by the control board ranging from 0V to 5V; at the output we have 2 wires that supply 5V and 0V and allow to supply the control board and 3 wires to supply and control the motor at the desired speed. Thus these drives can be used to control the speed of brushless motors using the adjustable output voltage of a programmable card [19].

3.3.2.3 Arduino card

An Arduino Nano board is a printed circuit board that provides access to all of the inputs and outputs of a microcontroller. Also included are a few other electronic components that can be used to operate or extend the microcontroller [25].

3.3.2.4 Module nRF24L01

nRF24L01 2.4 GHz radio module is a radio frequency transceiver module that operates on the 2.4 GHz band (such as Wi-Fi and Bluetooth). The thing that makes all of its beauty shine is that it is controlled in the simplest way possible. The SPI port on a Arduino can actually be used to take control of it [25].

The characteristics of the previous ingredients will be found in Appendix E

3.3.2.5 Battery

The batteries used for this type of realization have a large capacity Li-Polymer (Li-Po) 3S (3 cells equivalent to 11.1V) batteries (between 2000mAh and 5000mAh) which are reliable and more durable rechargeable batteries than small batteries [19].



Figure 3. 10. Battery Li-Polymer (Li-Po) 3S

3.3.2.6 RC Transmitter and Receiver

- **Radio control FlySky FS-i6**

Radio Control system (RCS) uses a radio signal to operate a distant device. A quad-copter consists of two parts, a receiver attached to the frame, and a transmitter that sends control signals to the receiver. These parts are used for manual flight of the quad-rotor. By converting the reference signal into radio waves, the transmitter sends the flight instructions. The receiver on the vehicle collects these signals and generates PWM values to drive the vehicle. To recognize the transmitter signals, the transmitter and receiver must be bounded together before the first flight. For the current purpose, a FlySky FS-i6 2.4 GHz radio control is used with six channels. According to specific stick movements, each channel of the RCS transmitter provides a throttle value in the range (1000-2000). It is necessary to calibrate the RCS to determine the desired operating range. The steps for RCS calibration will be well described later [18].



Figure 3. 11. Radio control FlySky FS-i6

- **Radio controller based on arduino and nRF24I01**

It is possible also to create our own radio control system, which has a 2.4GHz transceiver; we designed it to be a portable hand control case. It is based on the same principle of connection to the FlySky FS-i6 radio controller described in the previous section. To achieve this, we rely on the nRF24L01 radio module, which has an unobstructed transmission range of 1 km. We can control it through the Arduino nano board through the SPI port. We added two joysticks to control the quad-copter through the transmission channels predefined on the Arduino Nano board, using only four channels we can control the six degrees of freedom our quad-copter has, we can also add channels in order to control other operations that may be determined in the future. Programming of RCS system is based on two codec's for the transmitter and receiver. We relied on the C programming language available on the Arduino IDE software. The calibration of RCS is performed in the same way as the FlySky FS-i6 radio controller. Calibration steps are described later. It is preferred to develop our proper radio controller in order to minimize the cost. In fact radio controllers available in the stores are expensive.



Figure 3. 12. Radio controller based on arduino and nRF24I01

3.3.2.7 Ardupilot Mega (APM)

The Ardupilot Mega (APM) is an open source autopilot system based on the Arduino platform. It allows users to build their own autopilot software. APM can be used to design autopilots for fixed wing aircraft, multi-rotor vehicles, cars, and even boats.

In APM, there are three main groups of pins: outputs, inputs, and analogs. ESCs drive the motors using PWM signals from the outputs. RC receivers connected to the input. Analog channels can be used to integrate additional sensors, such as sonar and infrared rangefinders, and As a digital output. These analog pins can be configured based on the application. In addition to these pin kits, there are connector slots for GPS, wireless telemetry, power, and micro USB.

The APM is programmable with Arduino IDE and has 16 channels and a 10-bit A/D converter. It is powered by an ATMEGA 2560 processor. The system has a 4 megabyte data flash memory chip for logging data. The APM contains a six-degree of freedom MEMS IMU (MPU-6000) containing a 3 axis gyroscope To measure angular velocity , a 3 axis accelerometer To measure acceleration , and a temperature sensor. Furthermore, APM has a MEMS pressure

sensor/barometer (MS5611-01BA) that measures altitude, and a magnetometer that can be integrated internally or via an external compass [18].

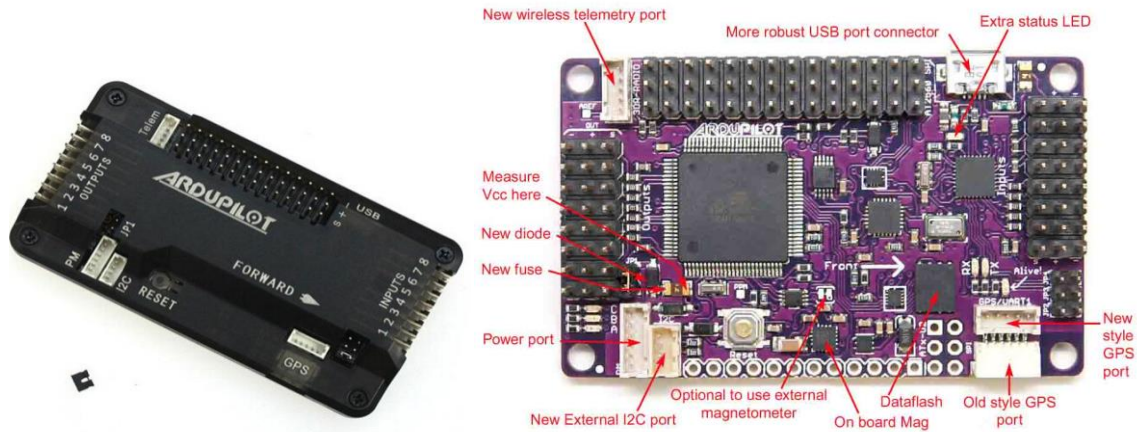


Figure 3. 13. Ardupilot Mega 2.8

3.3.3 Software used

During the software architecture phase, we used the necessary software that allowed us to configure and simulate our programs and our configurable components.

3.3.3.1 Mission planner

Mission Planner is an open-source program which can be used to serve as a virtual ground control station for helicopters, airplanes, and rovers. We can configure the various parameters of our autonomous device and ensure its optimal performance using this application.

Mission Planner is easy to install because the installation kit provides instructions. By opening the app, can connect it to the AutoPilot (Ardupilot) so can control the ground or air vehicle through the program.

Through it, we can create step-by-step missions for our gadget. We can begin by setting an origin point and specifying an elevation parameter. We can then input the mission's waypoints and other commands, depending on what we prefer the device to do. Figure 3.14 shows a Mission planner interface [26].



Figure 3.14. Mission planner interface

3.3.3.2 MATLAB software

MATLAB is used by engineers and scientists around the globe to analyze and design systems and products of the future. MATLAB is used in active safety auto systems, space vehicles, medical monitoring devices, and LTE mobile networks. Among its application areas are machine learning, signal processing, computer vision, communications, computational finance, controller design, robotics, and more.

MATLAB is designed for scientific and engineering applications. It is based on matrices, which is the most natural way to express computation mathematics. Data can be visualized easily with built-in charts. This is made possible thanks to a library of predefined charts. Here are some of the features of the software.

- A high-level programming language for scientific and technical computing.
- A desktop environment for iterative exploration, design, and problem solving.
- Charts for data visualization and tools for creating custom plots.
- Curve fitting, data classification, signal analysis, and many other specialized applications.
- Additional toolkits designed to meet the specific needs of engineers and scientists.
- A tool for creating applications with a customized user interface.
- Interfaces to C/C++, Java, .NET, Python, SQL, Hadoop and Microsoft Excel.
- MATLAB programs can be shared royalty-free with end users [26].

3.3.3.3 Arduino IDE

In Arduino IDE, you can program Arduino modules. Processing/Writing is the programming language used to implement the programming environment. The language includes many functions taken from C. Nonetheless, Arduino has its own set of libraries that are exclusive to this environment.

The advantage of being an open platform is that a license is not required, avoiding a considerable expense.

It offers the possibility of making any project that involves different inputs and, through an application developed in Arduino, it can be established a specific output [27].

3.3.4 Quad-copter setup

Setup and installation of a quad-copter are covered in this section. Utilizing all the components mentioned previously, the quad-copter is assembled and the autopilot is tested using Ardupilot Mission Planner GCS. The assembly of the frame begins by mounting the components on it and considering the load balancing, vibration damping, and component sensitivity.

For quad-copter, two configurations are available, X-configuration and +-configuration, in which the APM Board is mounted on the frame core to provide accurate orientation based on the user's control signals. APM Poor operation is caused by vibration. To achieve the necessary isolation, a thick layer of insulator is placed between the APM board and the frame core upper surface.

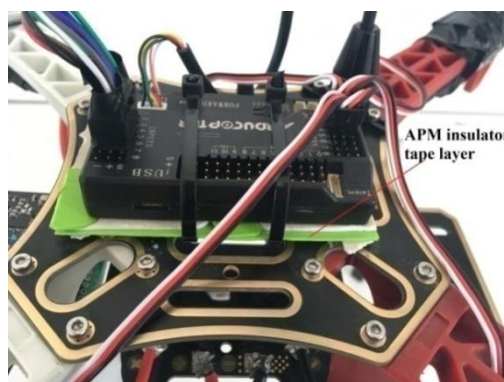


Figure 3. 15. APM insulation layer

The RC receiver is connected to the APM board, being placed next to it on the same core surface. There is a specific order in which the RC channels must be connected based on the intended operation. A nominal operation requires only four channels of the RC. The first channel controls the roll angle. In the second channel, control the pitch angle. The third channel is the throttle channel, which is used to set the desired altitude. The fourth channel is used to set the yaw. The receiver antenna it is almost parallel to the direction of the control signals.

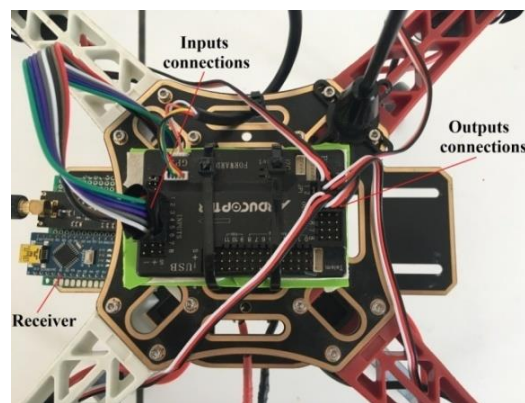


Figure 3. 16. APM Input and Output Connections

The LiPo battery is placed on the frame core lower surface which is the power distribution board. The ESC power cables are connected to a power distribution board, and the wires responsible for controlling the ESC are connected to the APM board. There are three wires in the motor which are power, ground and data. A similar order of wires is connected to the ESC high-power wires. The ESC provides the essential pulse widths to the motor through the data wire. In order to reverse the motor direction, the motor power and ground wires are swapped. The motors of each quad-copter diagonal must rotate in the same direction and motors of the different diagonals rotate in opposite directions, according to this, the propellers are mounted to specific motors according to their direction of rotation to provide the necessary lifting.

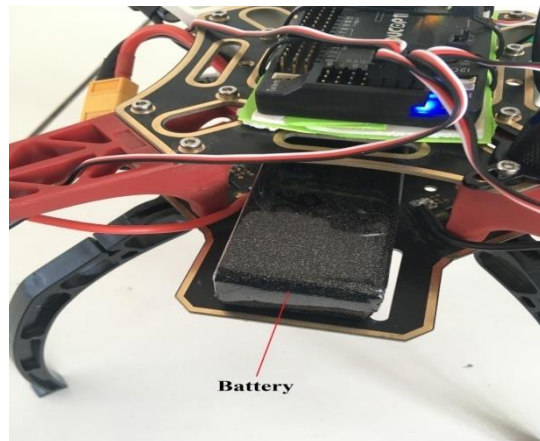


Figure 3. 17. Battery placement

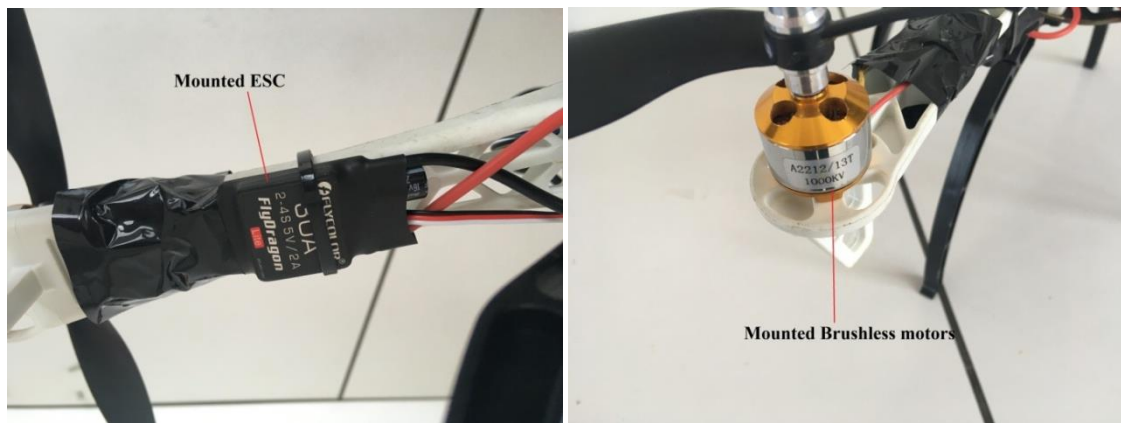


Figure 3. 18. Mounted ESC and brushless motor

If the installation is completed, a component calibration is performed. ESCs are individually calibrated. Then, the RC channel is calibrated to determine the desired pulse width range. The APM sensors (magnetometer and accelerometer) are calibrated for correct alignment. Calibration of the RC and sensor requires the use of mission planning software, and these calibration steps will be detailed later.

The first flight test is the final step in the setup, and APM mission planner GCS is used to perform it. The software is developed by the Ardupilot organization to control autonomous and non-autonomous vehicles from a ground station. For vehicle operation, the Mission planner provides firmware depending on the vehicle type. You can use an ArduCopter (multi-copter) or an Arduplane (plane) or an ArduRover (rover) to control your drone. APM software downloads and loads the ArduCopter firmware into the APM board. As soon as the firmware

is loaded, the quad-copter arming test can be performed to ensure that all components are connected and validated. Afterwards, a flight can be performed to ensure the quad-copter is ready for modifications. Modifications are made separately from the mission planner software and are mostly depend on code-based approaches.

3.3.5 Mechanism of operation

- **Configuration 1**

The following diagram shows how the design configuration of the drones based on the FlySky FS-i6 radio controller Figure 3.18. The various elements of this graph are:

1. Propeller
2. Brushless Motors
3. Bullet Connectors
4. ESC
5. Wiring harness
6. Lipo Battery
7. Battery Connectors
8. Ardupilot Board
9. GPS Module
10. Servo Connectors
11. Receiver
12. 2.4 GHz Antenna
13. Transmitter

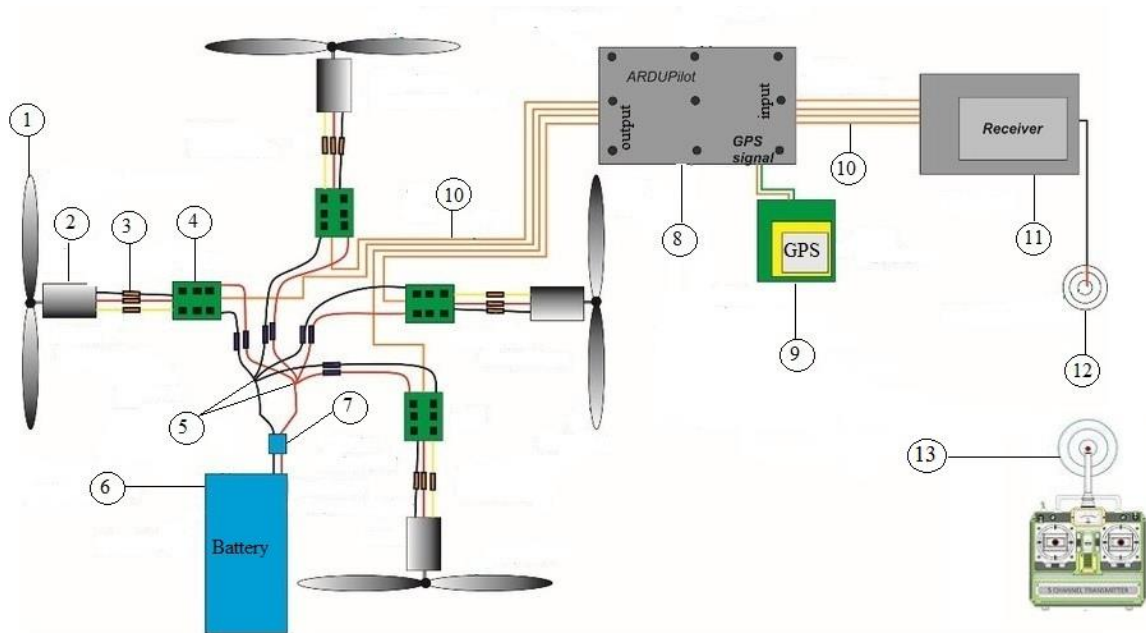


Figure 3. 19. Configuration 1 connection diagram

We have 04 ESCs and 04 motors, one ESC per motor. APM 2.8 board is connected to each ESC via an output pin.

There are 04 channels of the receiver, which are connected to 04 input pins of the APM 2.8. Battery power is provided to the 04 ESCs, which in turn supply power to the 04 motors and the ardupilot mega 2.8board. At the end of each motor is a propeller. Those on either side spin clockwise and those on the opposite side spin counterclockwise.

With the FS-i6 Radio Control, signals (commands) are sent to the receiver, which then communicates them to the APM 2.8, which in turn operates through the ESCs which control the speeds of the motors, and thus propeller rotation.

One of the ESCs provides power to both the ardupilot and the receiver on the drone. Some ESCs convert the voltage of the LiPo battery, which is greater than 5V, to a voltage of 5 VDC. Li-Po batteries are voltage-dependent depending on the number of cells they are made from. In our case, we used an 11.1 V DC battery.

- **Configuration 2**

The second configuration differs from the first in terms of transmitter and receiver. The transmitter and receiver in this configuration are based on the Arduino board and the nRF24L01 transceiver module. The following diagram shows how configuration 2 is designed Figure 3.19 and Figure 3.20 the various elements of this scheme are:

1. nRF24L01 Module
2. $100\mu F$ Capacitor
3. Arduino Nano Board
4. Switch ON/OFF
5. Battery
6. Joystick 2 Axis

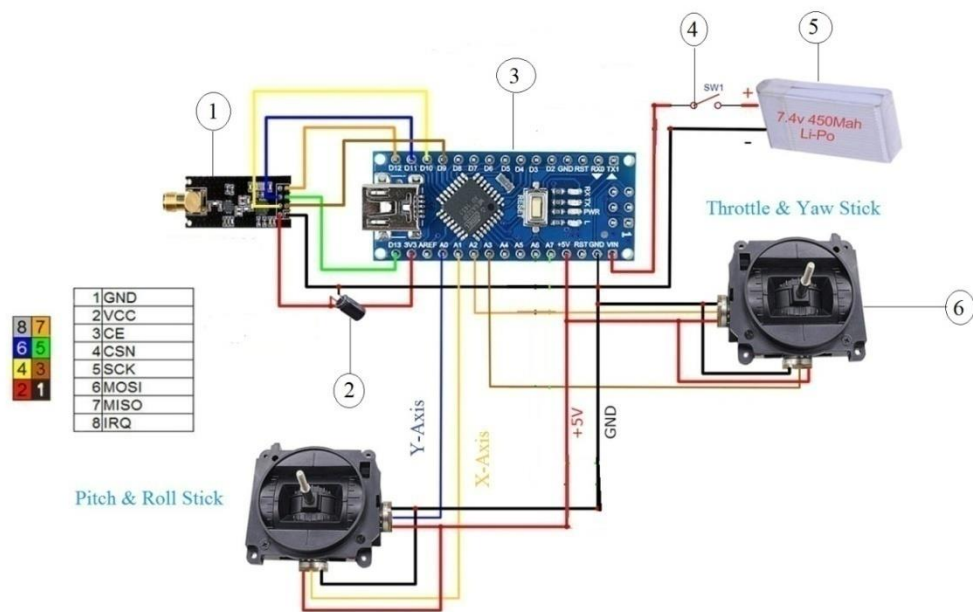


Figure 3. 20. Configuration 2 Transmitter Connection Diagram

3.3.6 The general (complete) structure of our quad-rotor drone



Figure 3. 22. The complete quad-copter structure

3.3.7 Components calibration

3.3.7.1 ESC calibration

Calibration of ESC is required for the first time. Calibrating an ESC involves specifying the PWM signal range. The ESC is calibrated only the first time. It remains calibrated until it is used another time with another range. As ESCs operate with APM board, there is either an automatic all-at-once calibration done by APM board or manual one-by-one calibration which is done independently of APM board.

The required components for calibration are:

- Fully charged LiPo battery.
- RC receiver and Transmitter.
- Single ESC and a motor.

Calibration steps

- ESC is connected to the throttle channel on the RC receiver.
- A high voltage wires from the ESC is connected to the motor.
- Transmitter is turned on and throttle stick is set to maximum.

- LiPo battery is connected to the ESC power cables.
- ESC releases two beeps. After these beeps, the throttle stick is lowered to its minimum position.
- By the end of the beeping sequence, the ESC will release a long beep. It indicates the ESC has finally been set to the desired range by the long beep.
- The battery is disconnected and so are the ESC control wires.
- Same method is applied to all other ESCs.
- Keep in mind that the RC receiver must be powered synchronously with the ESC; this can be done by utilizing the APM connection itself.

3.3.7.2 IMU sensors calibration

Accelerometers and internal compass sensors need to be calibrated in the IMU. There is no need to calibrate the gyroscope.

- **Accelerometer calibration:**

The accelerometer initially needs to be calibrated. For the first time, the accelerometer could not determine the direction of the quad-copter. Fortunately, there is an arrow at the top of the APM plate to easily identify the orientation of the plate as well as facilitate the calibration steps. Assuming the APM is installed in the direction of the arrow, it can be calibrated using the APM task planning software. APM is associated with the Mission Planner Program. The software details the calibration steps and assesses the correctness of the calibration process.



Figure 3. 23. Accelerometer Calibration

- **Internal compass calibration:**

Compass calibration is necessary because the developed code relies on a sensors fusion algorithm that uses the compass and GPS to determine attitude and altitude. Like the accelerometer, the compass must be calibrated the first time through the APM mission planning software. The software provides the necessary calibration steps and verifies the correctness of the calibration.

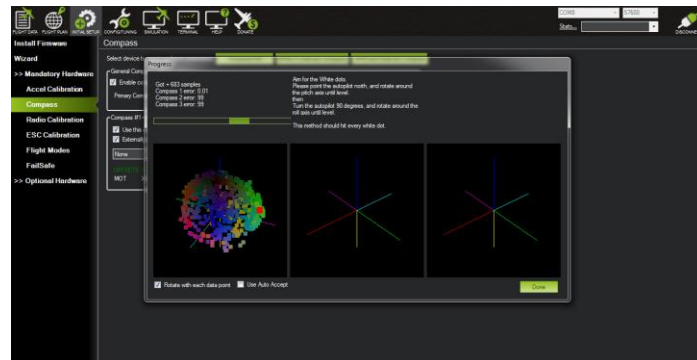


Figure 3. 24. Internal Compass Calibration

3.3.7.3 RC Calibration

Calibration can be done using an Arduino board or using the APM mission planning software for the APM board, as mentioned earlier. The APM Mission Planner calibration procedure is a more reliable technique. The APM is connected to the channels of the RC receiver. The Mission Planner software provides the necessary steps for RC calibration. During calibration, the joysticks must be placed in their maximum and minimum positions in order to record the endpoints of the PWM signal. At the end of the calibration, the APM mission planning software provides a table with all the channel endpoints reached. This table can be used to check the operation of the RC.



Figure 3. 25. RC Calibration

3.3.8 Field tests

For the flight test mission, we first hung the drone with the protective rope; this is for a safe flight test and to protect the drone from falling into instability. After several experiments and making sure of its stability during flight, we re-tested it without the protective rope as shown in the Figure 3.25.

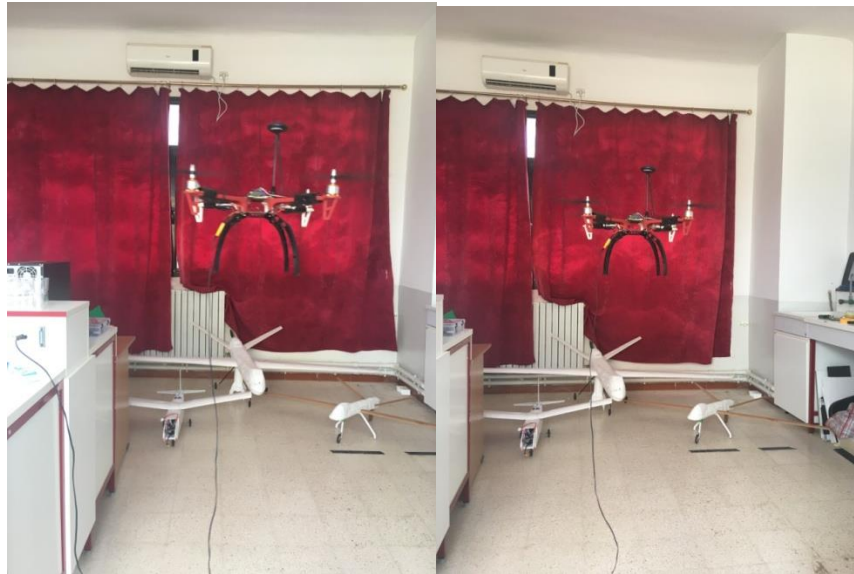


Figure 3. 26. Field tests

3.4 Conclusion

This chapter discusses the simulation results of PD and DSMC controllers, after which the elements used in designing the quad-copter system are introduced. Then the design of the radio control is explained. Next, we have provided details about the basic assembly that must be completed in advance, so that everyone can communicate. We then discussed how to calibrate a quad-copter, which we were able to test and found to be stable in flight.

General conclusion

In this project design and implementation of a drone is realized. This kind of project needs an important background about programming and automatic control.

This type of subject has been selected in order to improve our knowledge and skills about design and programming. For this purpose, quad-copter systems require a variety of knowledge, including mechanics, aviation, information technology, automation, electronics and communications. In this project, we developed a mathematical model of an aerobic vehicle, synthesized a stability control law based on discrete-time-slide mode control (DSMC). Theoretical modeling is validated by using Matlab's numerical simulation.

This work is divided into parts; the first one concerns a literature study of drone control technique and simulation using Matlab/simulink, the second one deal with the hardware realization using specific electronic components.

This work represents a big challenge

The obtained results concerning simulation demonstrate good efficiency of the control method used for controlling the quad-copter. The designed model of the drone is considered more stable. In fact, during the experiment tests of flying the drone keeps its stability. So, several experiments have been performed in the laboratory under specific conditions.

As a future work, collecting data in real time, using telemetry and other components is suggested. To implement the DSMC controller in practice for improving the stability of the quad-copter even in turbulent weather conditions is proposed.

Another important option to mention is the implementation of an obstacle avoidance system that can be implemented using a distance sensor, such as an infrared sensor, sonar or vision system.

An important improvement is being able to send the quad-copter to independent missions after defining the path we want them to take.

Bibliography



Bibliography

- [1] Arnaud KOEHL, “Modelisation, observation et commande d’un drone miniature a birotor coaxial,” Ecole doctorale IAEM Lorraine, 2012.
- [2] B. Sousa, “Estimation and Control of a Quadrotor Attitude ^ Engenharia Mec anica,” 2011.
- [3] C.A patel, “Building a Test Bed for mini Quadrotor Unmanned Aerial Vehicle with protective Shroud,” School of Wichita State, 2006.
- [4] K.M. Zemalache, “Commande d’un système sous-actionné : Application à un drone à Quatre Hélices,” d’Evry Val d’Essonne, 2005.
- [5] Amrani Mohamed Ounissi Nasreddine, “Etude et réalisation d’un drone quadrirotor,” Université 8 Mai 1945 – Guelma, 2020.
- [6] Heba talla Mohamed Nabil ElKholly, “Dynamic Modeling and Control of a Quadrotor Using Linear and Nonlinear Approaches,” The American University in Cairo (AUC), 2014.
- [7] Mark Willis Bailey, “Unmanned aerial vehicle path planning and image processing for orthoimagery and digital surface model generation,” 2012.
- [8] Farid Kendoul, “Survey of advances in guidance, navigation, and control of unmanned rotorcraft systems,” *F. Robot.*, vol. 29(2), 2012.
- [9] Anes BENMERZOUG Oussama MEKKID, “Commande et Navigation d’un Quadrirotor : Etude et Réalisation,” Ecole Nationale Polytechnique, 2016.
- [10] VICENTE MARTÍNEZ MARTÍNEZ Modelling, “Modelling of the Flight Dynamics of a Quadrotor Helicopter,” Cranfield University, 2007.
- [11] khebbache.H, “Tolérance aux défauts via la méthode backstepping des systèmes non linéaires Application : Système UAV de type Quadrirotor,” UNIVERSITE FERHAT ABBAS DE SETIF, 2012.
- [12] Somayeh Norouzi Ghazbi Ali Akbar Akbar Yasaman Aghli, “Quadrotors unmanned aerial vehicles: A review,” *Int. J. Smart Sens. Intell. Syst.*, vol. 9, 2016, doi: DOI: 10.21307/ijssis-2017-872 CITATIONS.
- [13] HASSENI Seif El Islam Soutene, “Commande Robuste Non-linéaire d’un Quadrotor,” Mohamed Khider – Biskra, 2020.
- [14] V. K. Mulgaonkar, Y., G. Cross, “Design of small, safe and robust quadrotor swarms,” 2015.
- [15] A. F. Tognon, M., A. Testa, E. Rossi, “Takeoff and landing on slopes via Inclined hovering with a tethered aerial robot,” 2016.

-
- [16] A. . R.-C. A. Kondak, K., K. Krieger, A. Albu-Schaeffer, M. Schwarzbach, M. Laiacker, I. Maza and Ollero, "Closed-loop behavior of an autonomous helicoptre equipped with a robotic arm for aerial manipulation tasks," *Adv. Robot. Syst.*, vol. 10(2), 2013.
- [17] A. F. Ryll, M., G. Muscio, F. Pierri, E. Cataldi, G. Antonelli, F. Caccavale, "6D physical interaction with a fully actuated aerial robot," 2017.
- [18] Amir Hussein, "Autopilot Design for a Quadcopter," Johns Hopkins University, 2017. [Online]. Available: <https://www.researchgate.net/publication/331298873>
- [19] Azouz Mustapha, "Modélisation et commande d'un quadrirotor : Etude comparative de la commande floue et PID," UNIVERSITE MOULOUD MAMMERI DE TIZI-OUZOU, 2016.
- [20] Randal Beard, "Quadrotor Dynamics and Control Rev 0.1," 2008.
- [21] Paul Pounds et al, "Design of a four-rotor aerial robot," in *Australasian Conference on Robotics and Automation*, 2002, p. 150.
- [22] Matko Orsag and Stjepan Bogdan, *Influence of Forward and Descent Flight on Quadrotor Dynamics*. Louis: February 24th, 2012, 2012. doi: 10.5772/2406.
- [23] Dounia Meradi, "A predictive sliding mode control for quadrotor's tracking trajectory subject to wind gusts and uncertainties," *Int. J. Electr. Comput. Eng.*, vol. 12, 2022, doi: DOI: 10.11591/ijece.v12i5.ppxx-xx.
- [24] Vincent Dabin, "COMMANDE D'UN QUADRICOPTÈRE PAR REJET ACTIF DE PERTURBATIONS," UNIVERSITÉ DE MONTRÉAL COMMANDE, 2018.
- [25] ELMAHARAT Anis LAKHDARI Raouf, "Conception et réalisation d'un mini drone," Université de Mohamed El-Bachir El-Ibrahimi - Bordj Bou Arreridj, 2021.
- [26] LAMRI Sofiane et MOHAMMEDI Achref, "Contribution à l'étude et réalisation d'un Quadrotor hybride UAV/UGV," HIGHER SCHOOL IN APPLIED SCIENCES --T L E M C E N--, 2020.
- [27] Miguel Ángel Granado Navarro, "Arduino based acquisition system for control applications," UNIVERSITAT POLITECNICA DE CATALUNYA, 2012.

Appendix



Appendix A

Rotation Matrix

First rotation

The first rotation is a rotation of ψ around the Z_0 axis which makes the Y_0 axis coincides with the Y' axis and the X_0 axis with the X' axis. The rotation matrix is given by the following equation.

$$R_\psi = \begin{bmatrix} \cos(\psi) & -\sin(\psi) & 0 \\ \sin(\psi) & \cos(\psi) & 0 \\ 0 & 0 & 1 \end{bmatrix}$$

Second rotation

The second rotation is a rotation of θ around the Y' axis which makes the X' axis coincide with the X axis and the Z_0 axis with the Z' axis. The rotation matrix is given by the following equation.

$$R_\theta = \begin{bmatrix} \cos(\theta) & 0 & \sin(\theta) \\ 0 & 1 & 0 \\ -\sin(\theta) & 0 & \cos(\theta) \end{bmatrix}$$

2.5.1 Third rotation

The third rotation is a rotation of φ around the X_I axis which makes the Z' axis coincides with the Z axis and the Y' axis with the Y_I axis. The rotation matrix is given by the following equation.

$$R_\varphi = \begin{bmatrix} 1 & 0 & 0 \\ 0 & \cos(\varphi) & -\sin(\varphi) \\ 0 & \sin(\varphi) & \cos(\varphi) \end{bmatrix}$$

Appendix B

Dynamic Model

Translation dynamics

According to Newton's second dynamic law in the inertial frame:

$$m \ddot{X} = \sum F_{ext}$$

Or:

$m \in \mathcal{R}^+$, is the total mass of the quad-rotor.

$X = \begin{bmatrix} x \\ y \\ z \end{bmatrix} \in \mathcal{R}^3$, is the position vector of the quad-rotor in the inertial frame.

$\sum F_{ext} \in \mathcal{R}^3$, is the vector of total external forces.

The external forces applied to the quad-rotor are:

The weight

It is the gravitational force of the earth. It is given by:

$$P = \begin{bmatrix} 0 \\ 0 \\ -m g \end{bmatrix}$$

with: $g \in \mathcal{R}^+$, is the acceleration of gravity on earth.

Thrust force

It is the total force generated by the rotation of the propellers of the four rotors. It is directed upwards, that is to say, it tends to lift the quad-copter. Given by:

$$F_p = Rot. \begin{bmatrix} 0 \\ 0 \\ T \end{bmatrix}$$

$T = \sum_{i=1}^4 f_i$ is the total thrust force of the four propellers.

f_i is the thrust force produced by the rotation of the propeller i , it is given by:

$$f_i = b \cdot \omega_i^2$$

with: $b \in \mathcal{R}^+$, thrust coefficient.

- **Rotational dynamics**

According to Newton's second law of dynamics

$$\frac{d(I\Omega)}{dt} = \sum \Gamma_{ext}$$

And as the angular velocity is expressed in the frame linked to the quad-rotor, then:

$$\frac{d(I\Omega)}{dt} = I\dot{\Omega} + \Omega \wedge I\Omega$$

The following expression is obtained.

$$I\dot{\Omega} = -\Omega I\Omega + \sum \Gamma_{ext}$$

with:

$$I = \begin{bmatrix} I_x & 0 & 0 \\ 0 & I_y & 0 \\ 0 & 0 & I_z \end{bmatrix} \in \mathcal{R}^{3 \times 3}, \text{ is the inertia matrix of the quadrotor.}$$

$\sum \Gamma_{ext} \in \mathcal{R}^3$, is the vector of external moments.

$$\Omega = \begin{bmatrix} p \\ q \\ r \end{bmatrix} \in \mathcal{R}^3, \text{ is the vector angular rates in the body-fixed frame.}$$

The external torques applied to the quad-copter is:

Aerodynamic torques

Aerodynamic torques is produced by the drag and thrust forces that are created by the rotation of the four propellers. They are given by:

$$\begin{cases} \tau_\varphi = l \cdot b (\omega_4^2 - \omega_2^2) \\ \tau_\theta = l \cdot b (\omega_3^2 - \omega_1^2) \\ \tau_\psi = k \cdot (-\omega_1^2 + \omega_2^2 - \omega_3^2 + \omega_4^2) \end{cases}$$

with:

$l \in \mathcal{R}^+$: represents the distance between the center of gravity of the quad-rotor and the axis of rotation of one of the rotors.

$b \in \mathcal{R}^+$: the thrust coefficient.

$k \in \mathcal{R}^+$: the drag coefficient.

Appendix C

Design of DSMC with Gao's reaching law

Second-order Slotine surface is defined as follows:

$$s_i[k] = e_{2i}[k] + \lambda_i e_{2i-1}[k], i = 1, 2, \dots, 6$$

In the following formula, $\lambda_i \in R^+$ are the constants of tuning, and $e[k]$ is the tracking error, which is the difference between the actual state $x[k]$ and the desired state $\tau[k]$.

$$e[k] = \begin{cases} e_{2i-1}[k] = \tau_{2i-1}[k] - x_{2i-1}[k] \\ e_{2i}[k] = \tau_{2i}[k] - x_{2i}[k] \end{cases}$$

$\tau[k]$ is the discrete-time of the trajectory that is desired

$\tau[t] = [x_d, \dot{x}_d, y_d, \dot{y}_d, z_d, \dot{z}_d, \varphi_d, \dot{\varphi}_d, \theta_d, \dot{\theta}_d, \psi_d, \dot{\psi}_d]^T \cdot \{x_d, y_d, z_d, \psi_d\}$ a trajectory generator will provide its derivatives, while $\{\varphi_d, \theta_d\}$ and its derivative can be deduced from the position controller.

Basically, the control is used to force the system to move on the sliding surface while keeping it from getting out, i.e.:

$$S = \{e[k] \mid s_i(e[k]) = 0, \quad i = 1, 2, \dots, 6\}$$

We introduce the virtual command $v_i[k]$ in such a way that $x_{2i}[k+1] = v_i[k]$, which gives us:

$$v_i[k] = x_{2i}[k] + h(f_i(x[k]) + g_i(x[k])u[k])$$

The dynamic of the surface is:

$$\begin{aligned} s_i[k+1] &= s_i[k] + e_{2i}[k+1] + \lambda_i e_{2i-1}[k+1] \\ &= s_i[k] + (\tau_{2i}[k+1] - v_i[k]) + \lambda_i e_{2i-1}[k+1] \end{aligned}$$

The Gao's reaching dynamics of the sliding surface are:

$$s_i[k+1] = (1 - h\sigma_i)s_i[k] - h\mu_i \text{sign}(s_i[k]), \quad i = 1, 2, \dots, 6$$

where σ_i and μ_i are tuning parameters and satisfying $0 \leq h\sigma_i < 1$ and $\mu_i > 0$.

The following virtual command signal is obtained:

$$v_i[k] = \sigma_i s_i[k] + \mu_i \text{sign}(s_i[k]) + \lambda_i e_{2i-1}[k+1] + \tau_{2i}[k+1], \quad i = 1, 2, \dots, 6$$

The discontinuous sign function causes chattering that needs to be addressed. It can be replaced by the following pseudo-sign function:

$$\text{psign}(x, \eta) = \frac{x}{|x| + \eta}$$

Where $0 < \eta \ll 1$ was chosen equal to (0,05).

The next step will be to determine the real command $u[k] = [u_1[k], u_2[k], u_3[k], u_4[k]]^T$ from $v_i[k]$.

$$\begin{bmatrix} v_x[k] \\ v_y[k] \\ v_z[k] + g \end{bmatrix} = \frac{U_1[k]}{m} \begin{bmatrix} c_{x7}[k]s_{x8}[k]c_{x9}[k] + s_{x7}[k]s_{x9}[k] \\ c_{x7}[k]s_{x8}[k]s_{x9}[k] - s_{x7}[k]c_{x9}[k] \\ c_{x7}[k]c_{x8}[k] \end{bmatrix}$$

$$\begin{bmatrix} v_\varphi[k] \\ v_\theta[k] \\ v_\psi[k] \end{bmatrix} = \begin{bmatrix} \left(\frac{I_y - I_z}{I_x}\right) x_{11}[k]x_{12}[k] \\ \left(\frac{I_z - I_x}{I_y}\right) x_{10}[k]x_{12}[k] \\ \left(\frac{I_x - I_y}{I_z}\right) x_{10}[k]x_{11}[k] \end{bmatrix} + \begin{bmatrix} \frac{U_2[k]}{I_x} \\ \frac{U_3[k]}{I_y} \\ \frac{U_4[k]}{I_z} \end{bmatrix}$$

to determine the $U_1[k]$, we notice that:

$$\frac{U_1[k]}{m} \begin{bmatrix} c_{x7}[k]s_{x8}[k]c_{x9}[k] + s_{x7}[k]s_{x9}[k] \\ c_{x7}[k]s_{x8}[k]s_{x9}[k] - s_{x7}[k]c_{x9}[k] \\ c_{x7}[k]c_{x8}[k] \end{bmatrix} = \frac{U_1[k]}{m} \cdot \text{Rot}$$

According to the properties of rotation matrices, we know that:

$$\left\| \frac{U_1[k]}{m} \cdot \text{Rot} \right\| = \left\| \frac{U_1[k]}{m} \right\|$$

Appendix D

Table D. 1. Quad-copter Parameters

Parameter	Value	Unit
m	1,05	Kg
I_x	0,01122	Kg.m ²
I_y	0,01122	Kg.m ²
I_z	0,02199	Kg.m ²

Table D. 2. Position Parameters of the PD Controller

Position	PD controller	
	K_p	K_d
X-Axis	12.37	3.5
Y-Axis	3.5	12.37
Z-Axis	20	5

Table D. 3. Angle Parameters of the PD Controller

Angle	PD controller	
	K_p	K_d
Roll	70	26
Pitch	70	41
Yaw	25	20

Table D. 4. Parameters of DSMC with Gao's reaching law controller



i	DSMC with Gao's reaching law controller		
	λ_i	σ_i	μ_i
1	2	1	9
2	5	1	0.5
3	10.5	1.1	5
4	8	10	9
5	8	3.2	9
6	9	1	5



Table D. 5. Parameters of DSMC with power rate reaching law controller


i	DSMC with power rate reaching law controller			
	λ_i	σ_i	μ_i	η_i
1	2	1	9	0.1
2	5	1	0.5	0.01
3	10.5	3	2	0.9
4	8	10	9	0.01
5	8	3.2	9	0.01
6	9	1	5	0.6

Appendix E

Components specification

Components	Specification	Figure
Frame DJIF450.	Diagonal Wheelbase: 450 mm. Frame Weight : 282 g. Takeoff Weight:800 g ~ 1600 g.	
Propellers.	Diameter: 10" (25.4 cm). Pitch: 4.5" (11.43 cm). Material : ABS.	1045 
Brushless motors 1000KV A2212/13T.	KV: 1000 RPM/V. Max Efficiency: 80%. Max Efficiency Current: 4 - 10A (>75%). Resistance: 0.090 ohms. Max Current: 13A for 60S. Max Watts: 150W. Weight: 52.7 g / 1.86 oz. Size: 28 mm dia x 28 mm bell length. Shaft Diameter: 3.2 mm. Poles: 14.	

<p>Electronic Speed Controller (ESC) / FlyDragon</p>	<p>Continuous current: 30A. Instantaneous current (10s): 40A. BEC: 5V/2A. Weight: 25g Size: 49×25.5×10.5mm</p>	
<p>Arduino Nano card</p>	<p>Microcontroller: ATmega328P – 8-bit AVR family microcontroller. Operating Voltage: 5V. Recommended Input Voltage for Vin pin: 7-12V. Analog Input Pins: 6 (A0 – A5). Digital I/O Pins: 14 (Out of which 6 provide PWM output). DC Current on I/O Pins: 40 mA. DC Current on 3.3V Pin: 50 mA. Frequency (Clock Speed): 16 MHz. Communication: IIC, SPI, USART.</p>	

Module nRF24L01	<p>2.4GHz RF transceiver Module.</p> <p>Operating Voltage: 3.3V.</p> <p>Nominal current: 50mA.</p> <p>Range: 1000 m.</p> <p>Operating current: 250mA (maximum).</p> <p>Communication Protocol: SPI.</p> <p>Baud Rate: 250 kbps - 2 Mbps.</p> <p>Channel Range: 125.</p> <p>Maximum Pipelines: 6.</p> <p>Low cost wireless solution.</p>	 The image shows an nRF24L01 2.4GHz RF transceiver module. It consists of a small black printed circuit board (PCB) with several surface-mounted components, including a microcontroller and various passive components. A gold-colored SMA connector is visible on the board. A long, black, flexible antenna is attached to the board via a small connector. The module is shown against a white background.
-----------------	---	--